CTEQ-TEA for JLab22: sea and valence partonic structure

Aurore Courtoy — for the CT collaboration
with Y. Fu, T. Hobbs, P. Nadolsky & C.-P. Yuan

Instituto de Física
National Autonomous University of Mexico (UNAM)

JLab22 meeting

01/23/23

The CTEQ-Tung et al (CT) PDF set

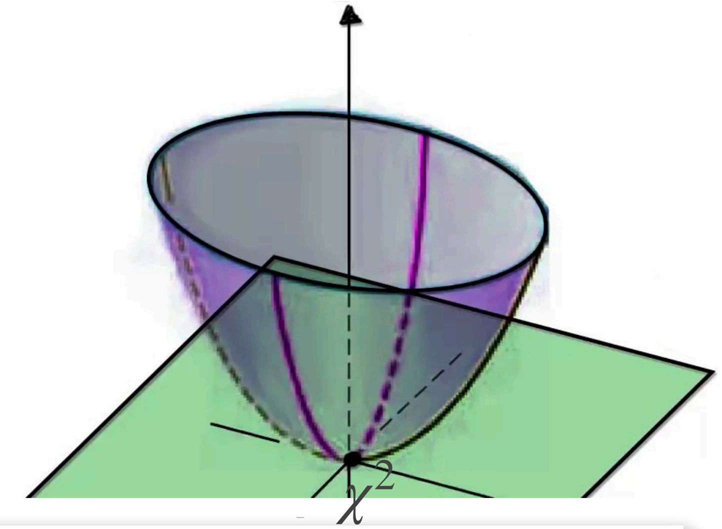

CT18NNLO is the general-purpose PDF set published in 2019.

[Hou et al, Phys.Rev.D 103 (2021)]

CT methodology is based on minimizing a χ^2 expressed in terms of *parametrizations* for the PDFs, finding the global minimum, and providing Hessian error PDFs to estimate the uncertainty.

The analysis is carried out at NNLO, and involves all essential data sets from various experiments.

CT's initial scale is $Q_0 = 1.3$ GeV.

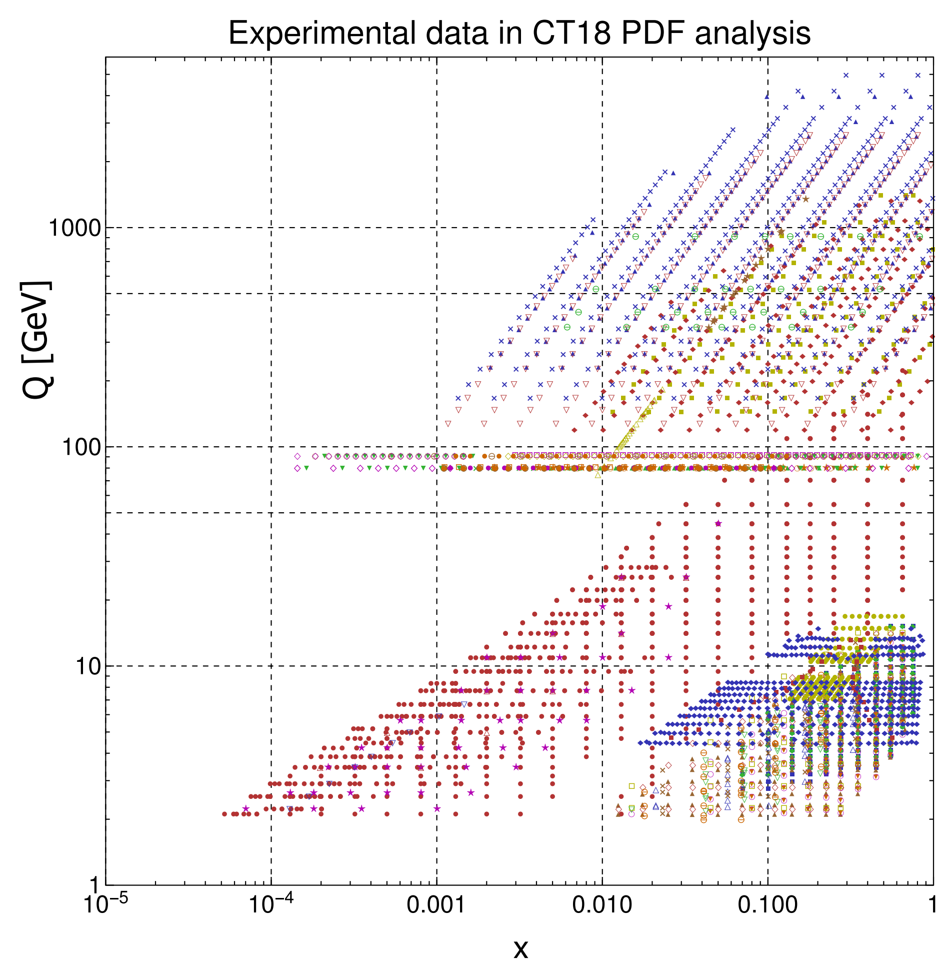

Latest kinematic coverage for CT18
3681 data points from over 39 different experiments
$Q > 2$ GeV and $W^2 > 12.25$ GeV^2.

The CTEQ-Tung et al (CT) PDF set

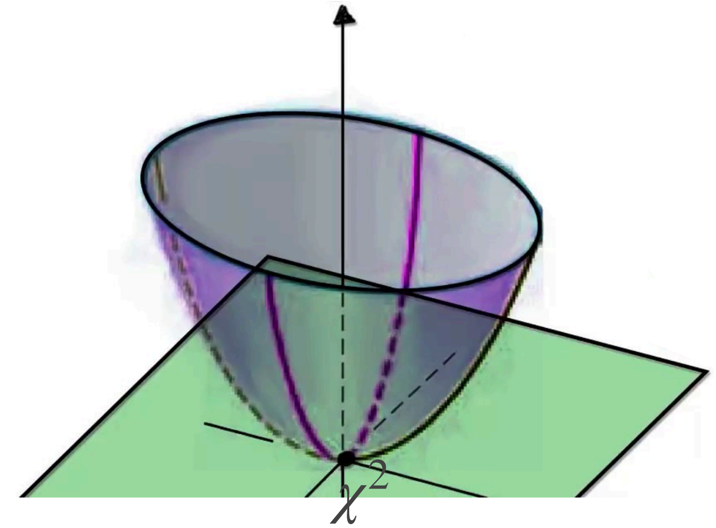

CT18NNLO is the general-purpose PDF set published in 2019.

[Hou et al, Phys.Rev.D 103 (2021)]

CT methodology is based on minimizing a χ^2 expressed in terms of *parametrizations* for the PDFs, finding the global minimum, and providing Hessian error PDFs to estimate the uncertainty.

The analysis is carried out at NNLO, and involves all essential data sets from various experiments.

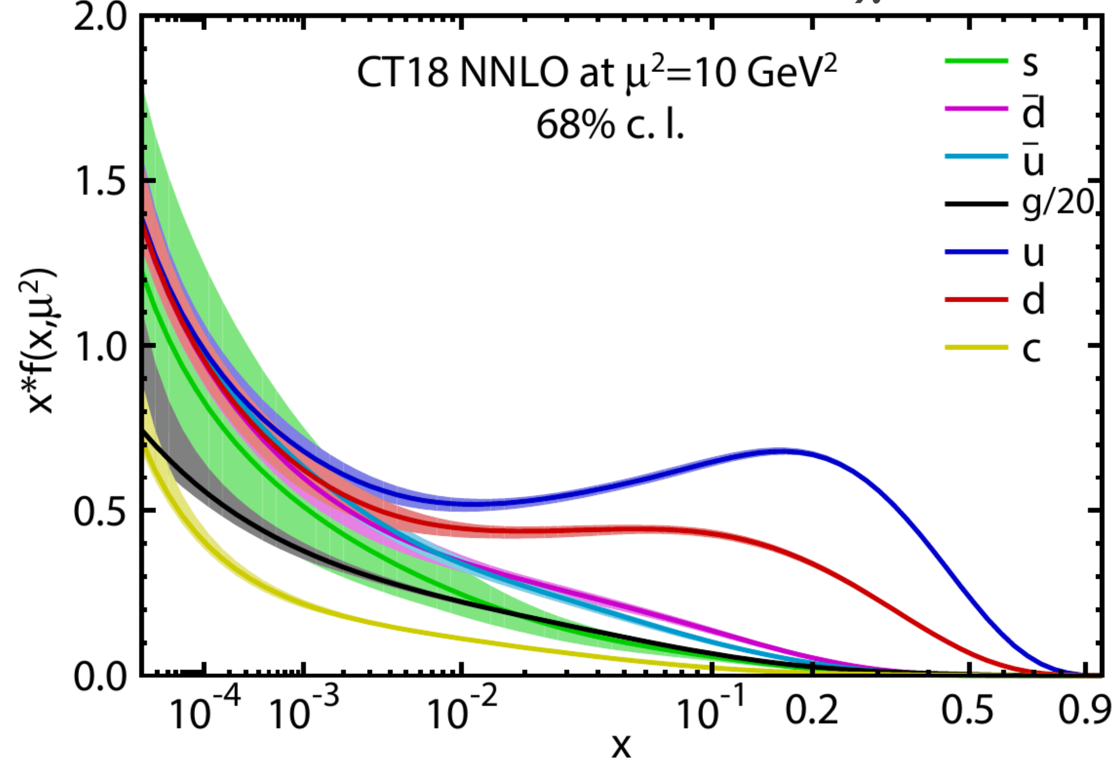

The CT18 family.

CT has released various specialized sets from studies of specific physics questions:

- strangeness asymmetry: CT18As

[Hou et al, 2211.11064]

- inclusion of lattice input for $s - \bar{s}$: CT18As_lat
- CT18FC: no evidence for fitted (intrinsic) charm in light of thoroughly estimated uncertainties

[Guzzi et al, 2211.01387]

Study of uncertainties

Tools to explore and understand the spread of uncertainties in PDF analyses.

The Hessian formalism allows for unique tools to visualize pulls from various experiments.

[Wang et al, PRD98]
[Hobbs et al., PRD100]

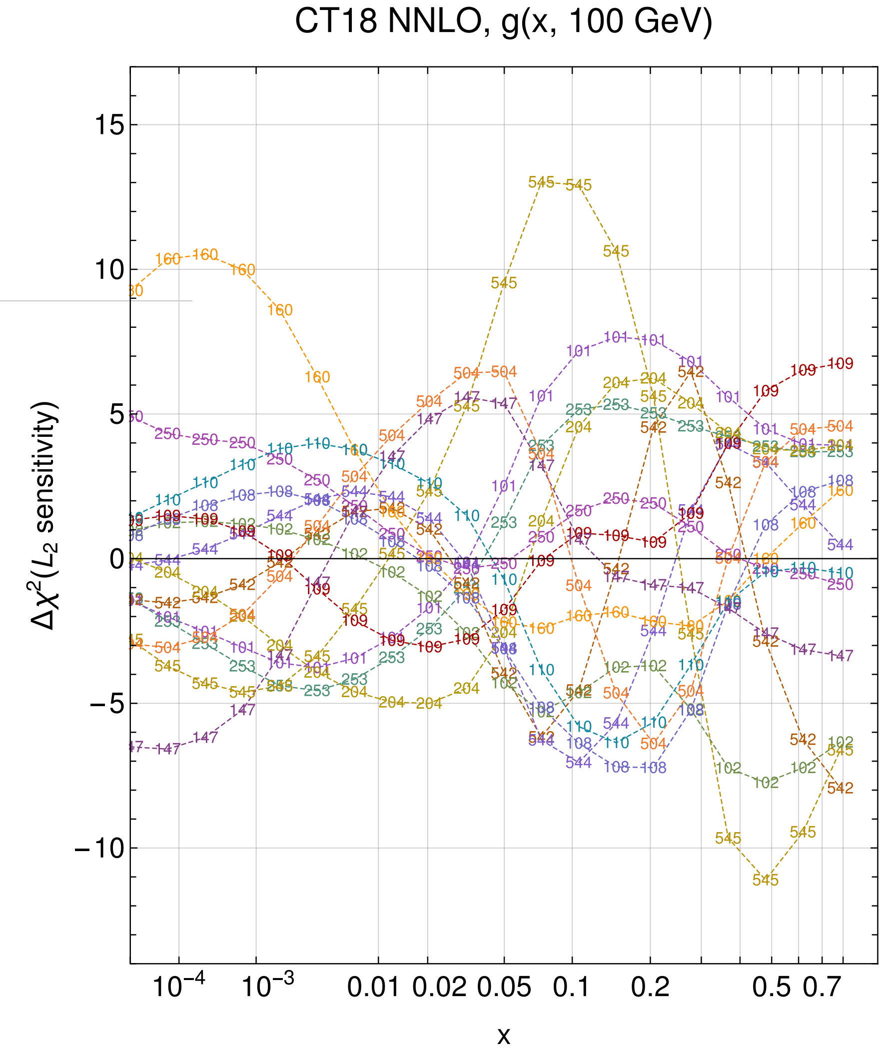

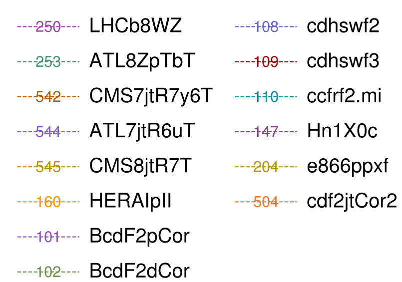

The CT formalism also allows to explore the space of PDF solutions and **reliably estimate PDF uncertainties.**

[Courtoy et al, to appear in PRD]

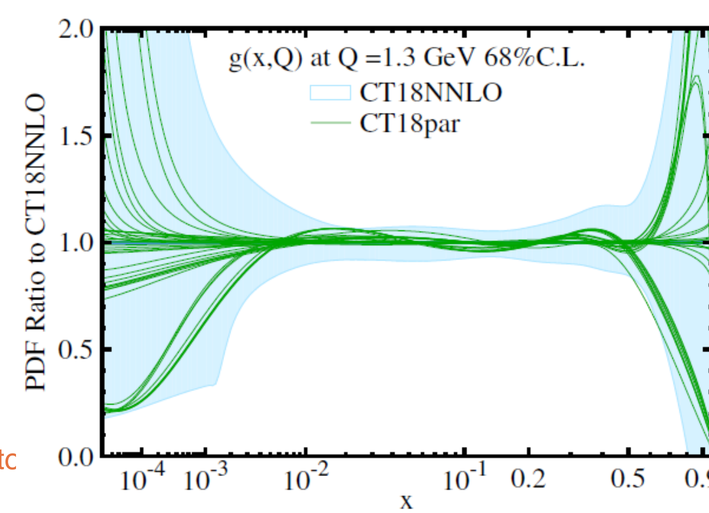

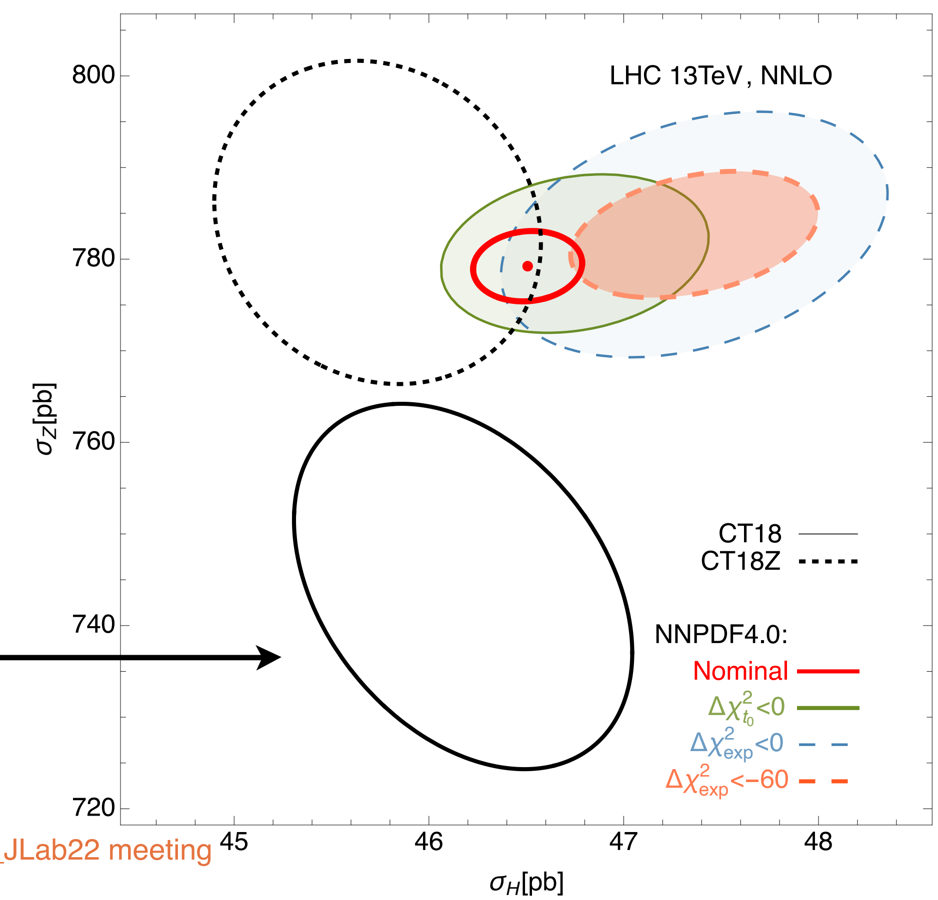

Flavor separation

Flavor separation in the sea is not well constrained at large x. Pheno large-x regime means $x \gtrsim 0.3 - 0.4$.

In CT's *low-sea* scenario for the sea, the sea PDFs are much smaller than the valence PDF for low Q^2 and $x > 0.2$. Other *high-sea* scenarios are possible, but require unusual unsmooth shapes for the sea PDFs.

$\Rrightarrow$ need to further constrain the sea PDFs at large x.

Flavor separation could be improved with, *e.g.*, more data constraints on $u - \bar{u}$ and $d - \bar{d}$ for $x \to 1$.

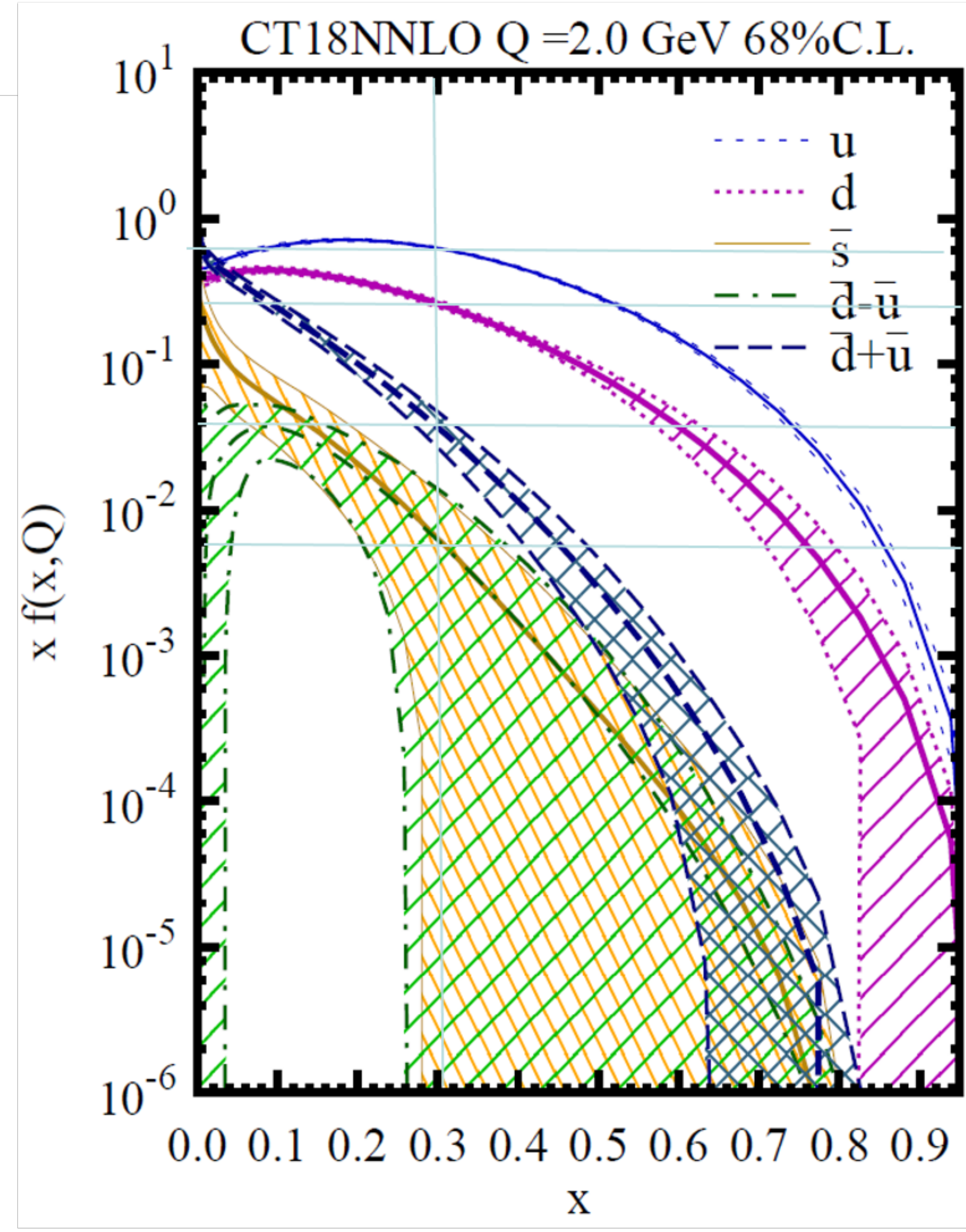

Flavor separation

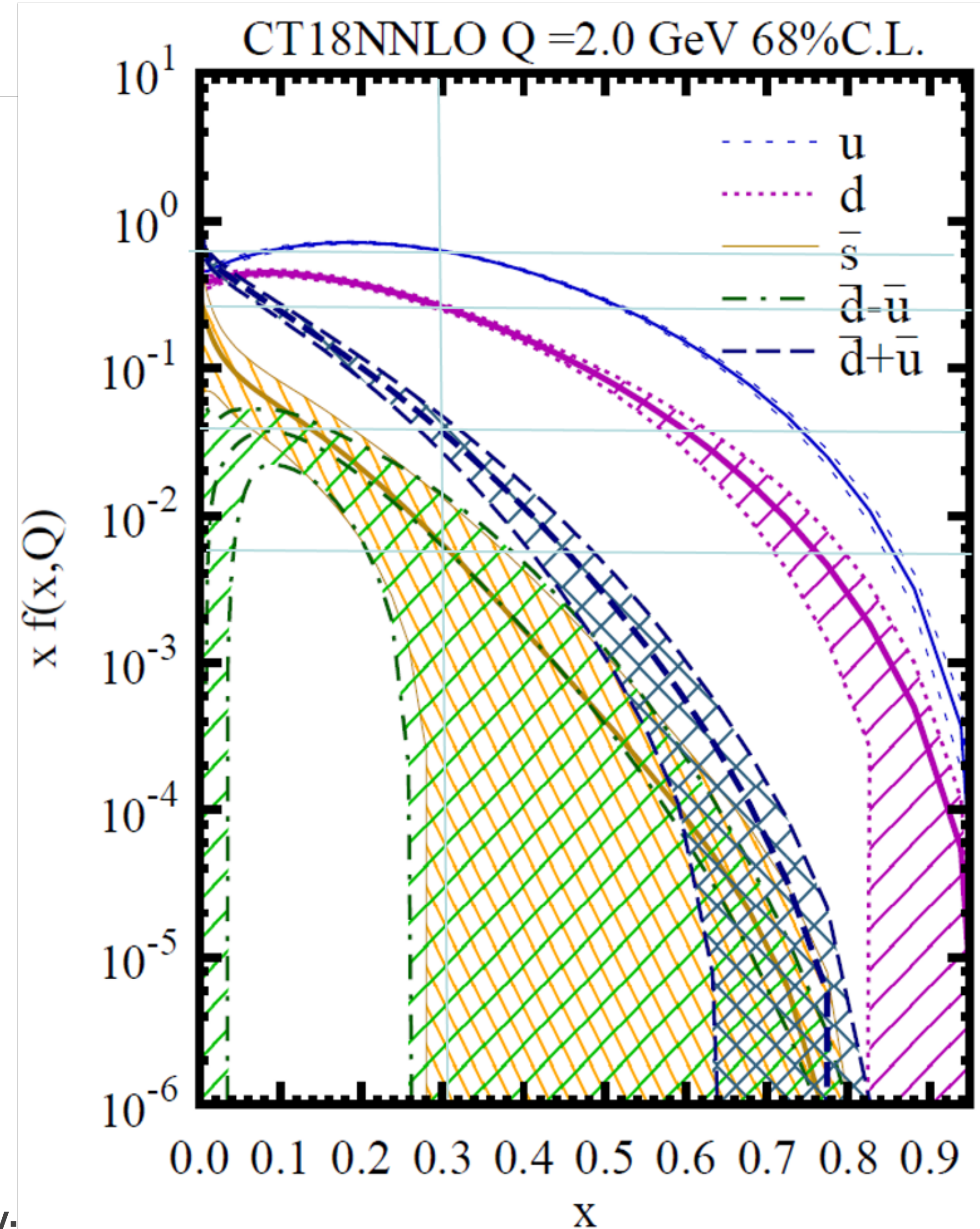

Flavor separation in the sea is not well constrained at large x. Pheno large-x regime means $x \gtrsim 0.3 - 0.4$.

In CT's *low-sea* scenario for the sea, the sea PDFs are much smaller than the valence PDF for low Q^2 and $x > 0.2$. Other *high-sea* scenarios are possible, but require unusual unsmooth shapes for the sea PDFs.

⤃ need to further constrain the sea PDFs at large x.

Flavor separation could be improved with, *e.g.*, more data constraints on $u - \bar{u}$ and $d - \bar{d}$ for $x \to 1$.

How we propose this can be achieved with JLab at 22 GeV:

I. constrain large-x PDFs at a low-Q energy from data at high x, such as LHC forward-backward asymmetry in Drell-Yan pair production.
II. systematic tools to predict leading-power PDFs at low Q^2, *i.e.*, to separate higher twists.

JLab @ 22GeV — kinematics

Our estimates for JLab 22 GeV:

[Owens et al, PRD87]
[Accardi et al, EPJC81]

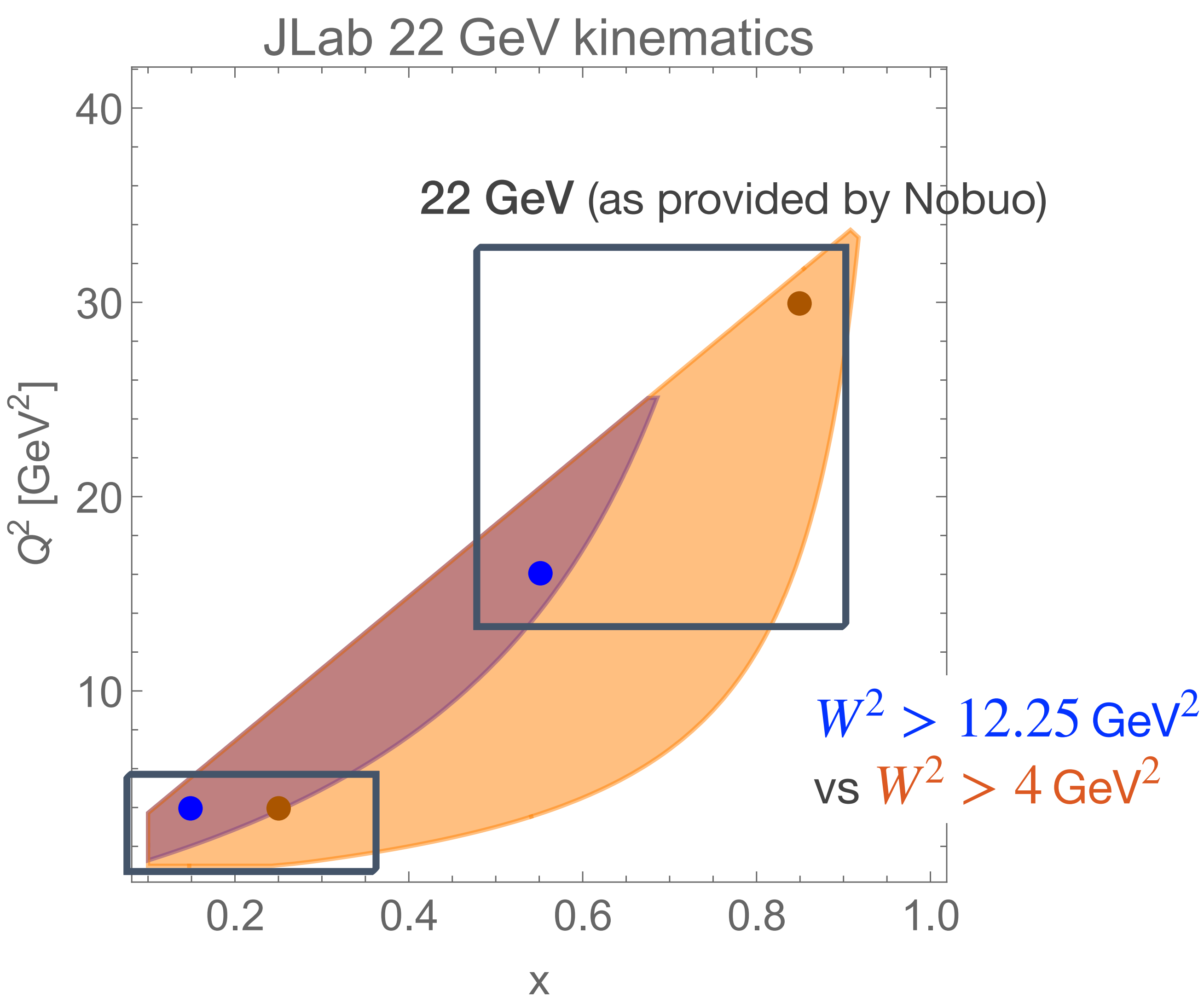

11 GeV (as provided by Nobuo)

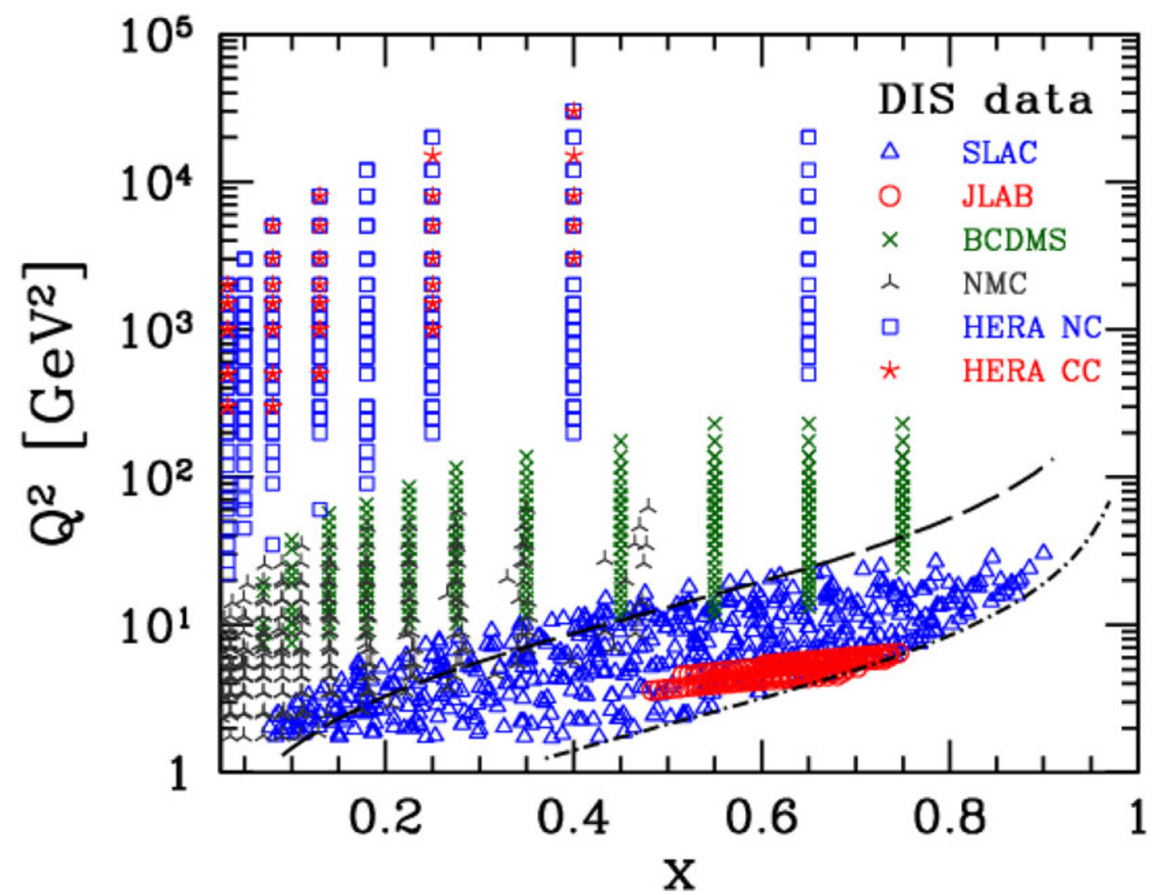

Old kinematic coverage showing the impact of the W^2 cuts on data selection.

Forward-backward asymmetry

NEW:
based on predictions from Fu, Hou, Yuan, et al.

Drell-Yan backward-forward dilepton production is sensitive to light sea and gluon for increasing M_{ll}.

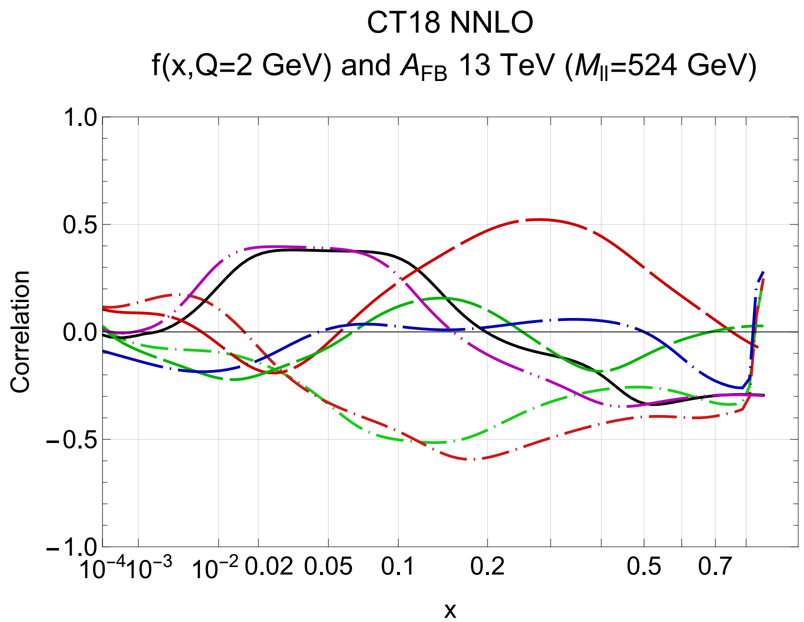

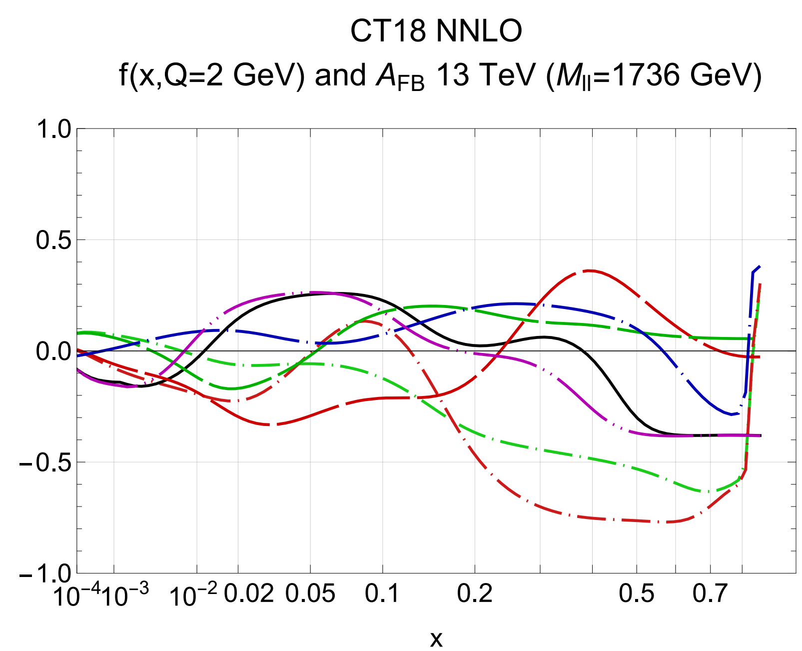

Strong anti-correlation of AFB with $\bar{u}$ and $\bar{d}$ (and gluon) at large x for increasing M_{ll}.

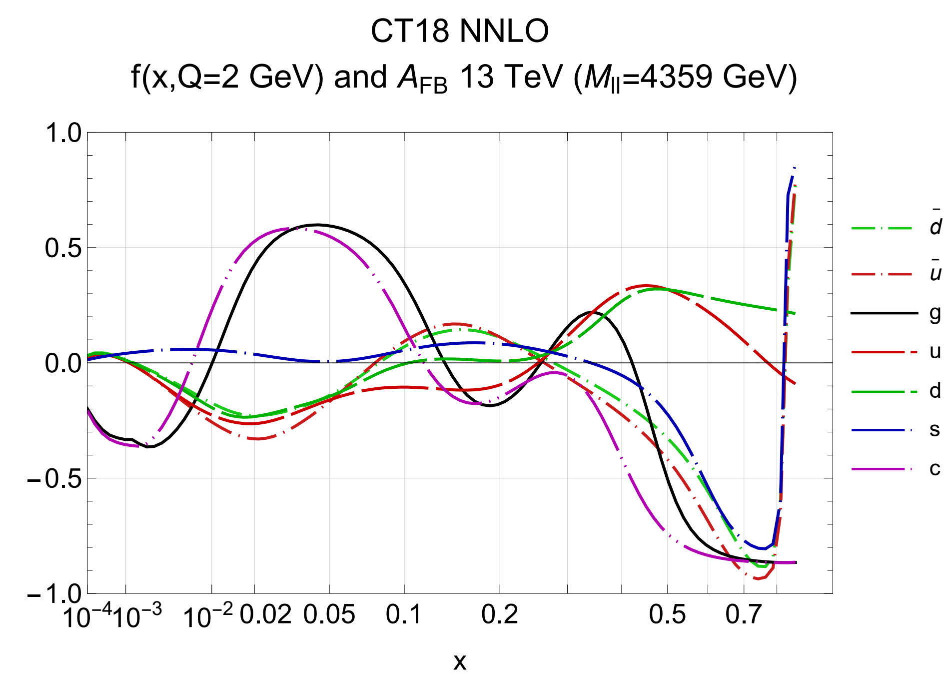

PRELIMINARY

Growing correlation of AFB with gluon at $x < 0.2$.

see also [Ball et al, EPJC 2022 82]

Large-x PDFs

The CT group has explored the role of quark-counting rules on PDF global analyses.

[Courtoy & Nadolsky, PRD103, 2112.14329]

The effective fall-off of the valence PDFs follows an approximate $(1-x)^{3+\Delta\beta}$ where $\Delta\beta$ is the variation due to DGLAP and hadronic corrections.

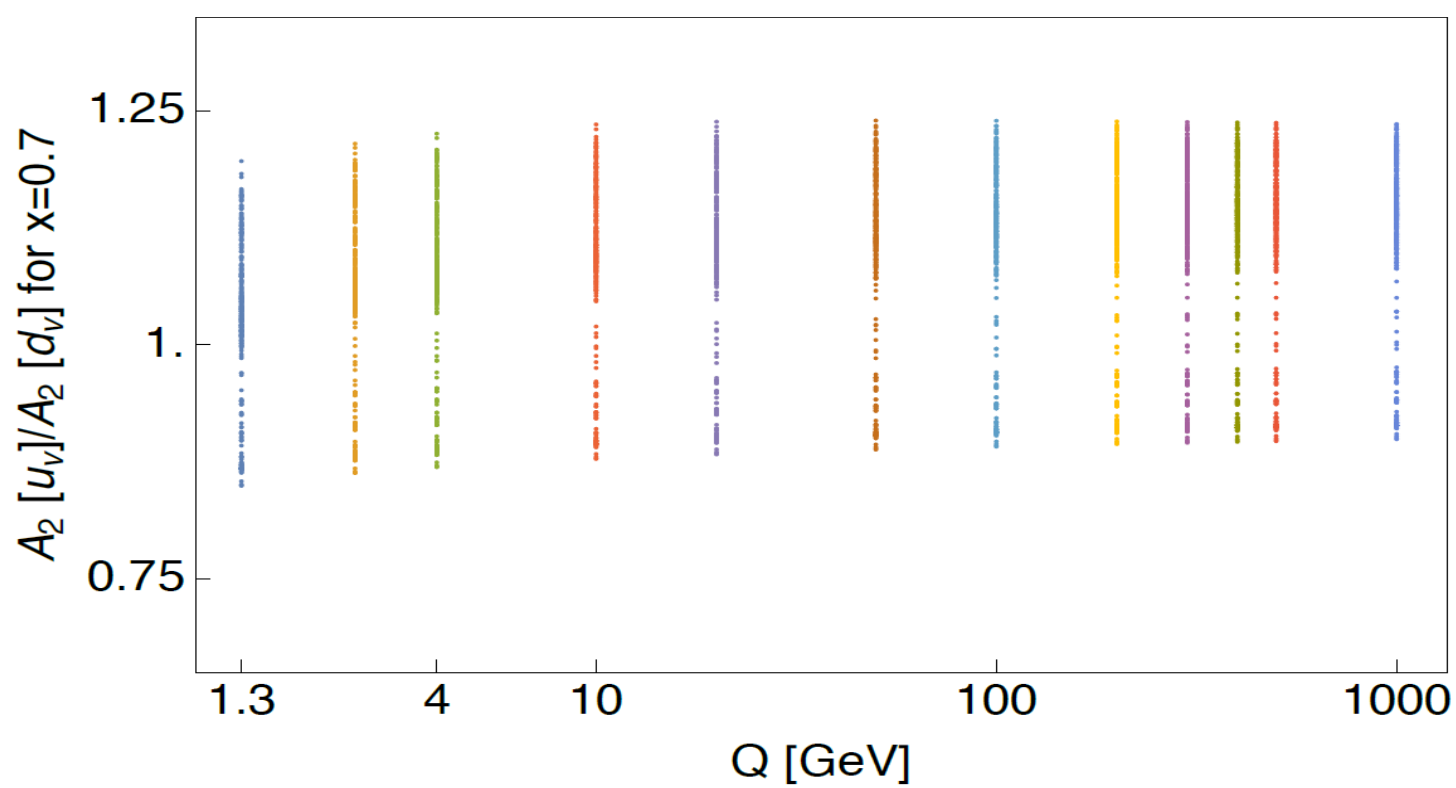

$$A_2^{\rm eff}(F) \equiv \frac{\partial \ln\left(F(x,Q)\right)}{\partial \ln(1-x)}$$

363 CT18NNLO replicas shown at given Q values

The ratio of effective exponents for valence PDFs is approximately independent of Q.

ZEUS data at large (x, Q^2) to be considered in the future *[Abt, PRD101]*.

Toward lower Q^2

Mid-Q^2 analyses encounter additional radiative contributions:

- ⇨ target mass corrections
- ⇨ higher-twist corrections — $\mathcal{O}(M^2/Q^2)$
- ⇨ nuclear corrections

Large-x PDFs determined from high Q^2 offer a possibility to systematically test the leading-power PDFs toward lower Q^2.

CT has studied the impact of various corrections, by analyzing CT vs. CJ (highlight on deuteron corrections), or examining the quark counting rules at mid-Q^2.

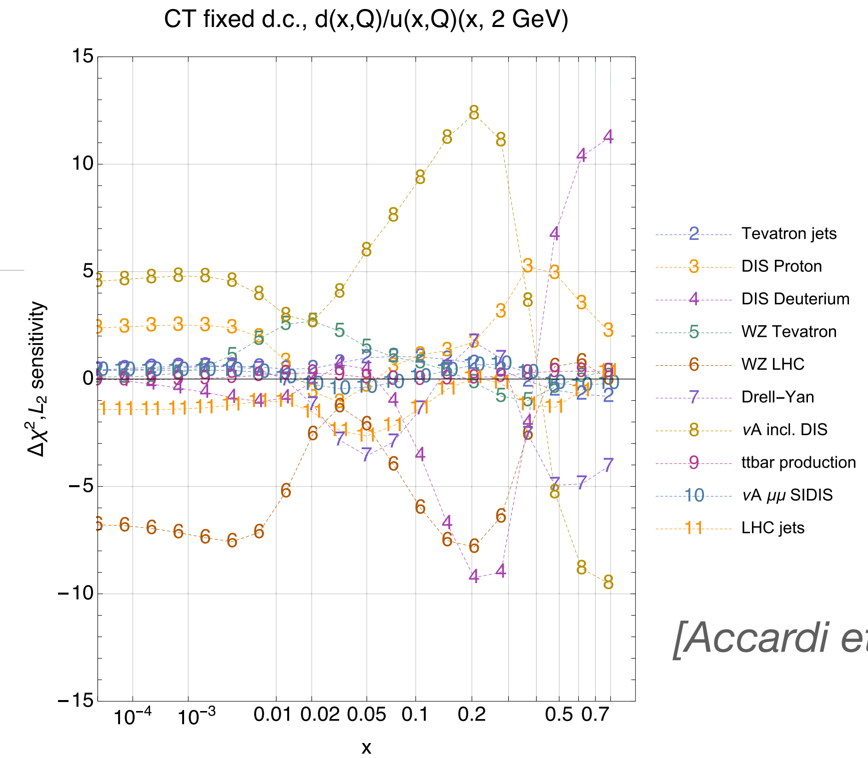

[Accardi et al, EPJC81]

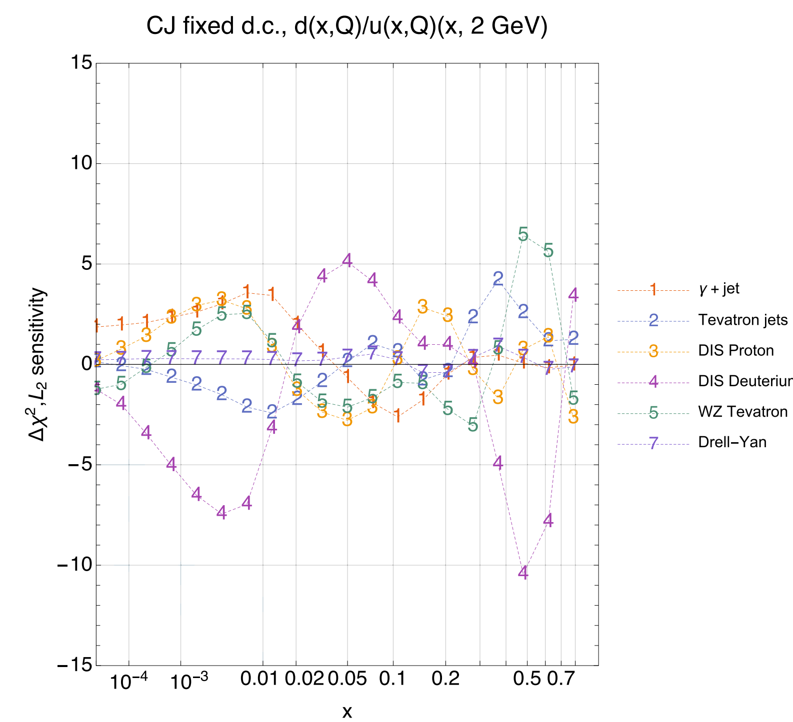

Pulls affected by cuts, *e.g.,* on deuteron data sets

L_2 sensitivity shows the correlation between a given PDF configuration and objective function.
Pulls on χ^2 when $f(x) \to f(x) + \Delta f(x)$.

Toward lower Q^2

Mid-Q^2 analyses encounter additional radiative contributions:

- ⇨ target mass corrections
- ⇨ higher-twist corrections — $\mathcal{O}(M^2/Q^2)$
- ⇨ nuclear corrections

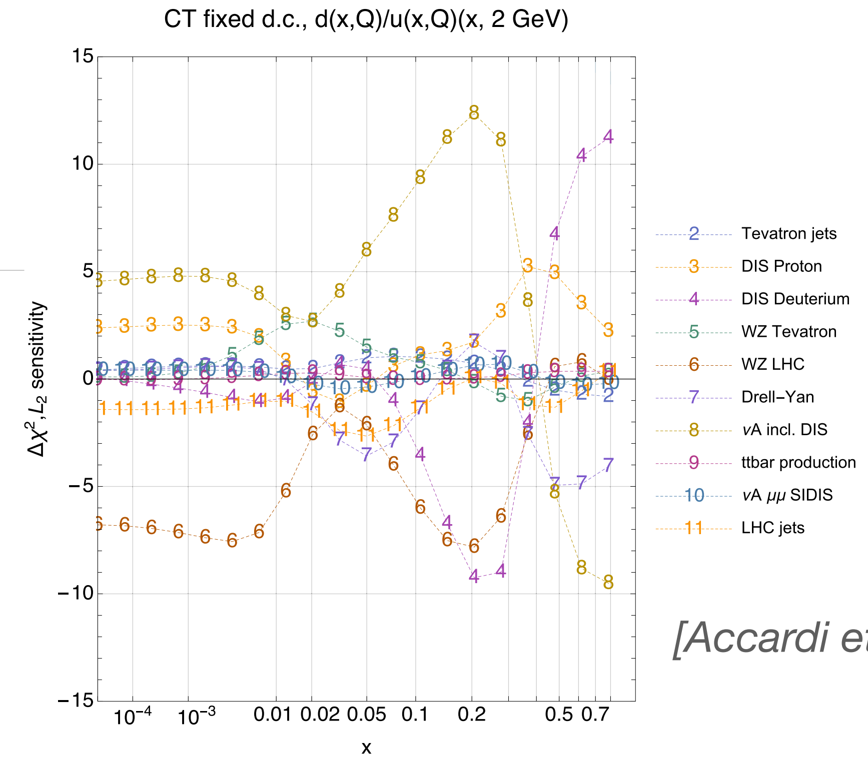

[Accardi et al, EPJC81]

Large-x PDFs determined from high Q^2 offer a possibility to systematically test the leading-power PDFs toward lower Q^2.

CT has studied the impact of various corrections, by analyzing CT vs. CJ (highlight on deuteron corrections), or examining the quark counting rules at mid-Q^2.

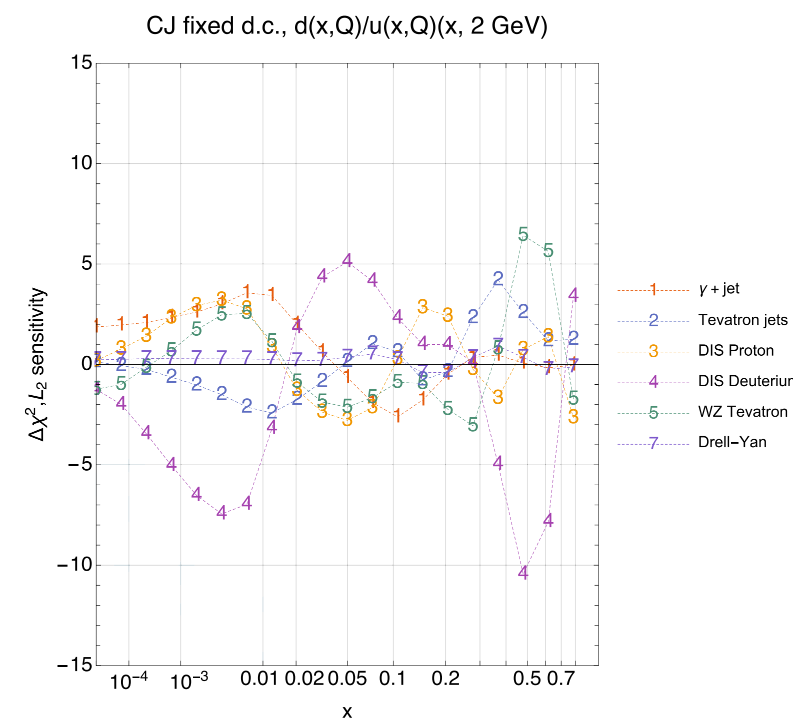

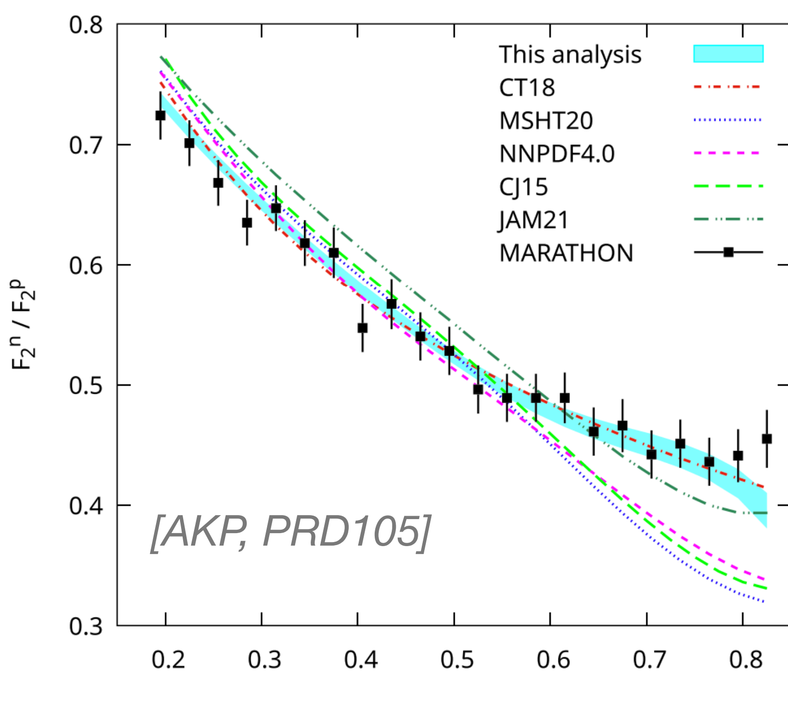

Pulls affected by cuts, *e.g.,* on deuteron data sets

L_2 sensitivity shows the correlation between a given PDF configuration and objective function.
Pulls on χ^2 when $f(x) \to f(x) + \Delta f(x)$.

Impact on parity-violating DIS —A_{PV}

APV at high energies: asymmetry holds to all orders in pQCD

$\rightarrow$ evaluate as twist-2 at (N)NNLO; constrain PDF uncert., BSM in couplings

at low(er) energies (including JLab20+), complex power-suppressed corrections; *e.g.*,

$$A^{\rm PV} = -\left(\frac{G_F Q^2}{4\sqrt{2}\pi\alpha}\right)\left[g_A^e \; Y_1 \; \frac{F_1^{\gamma Z}}{F_1^{\gamma}} + \frac{g_V^e}{2} \; Y_3 \; \frac{F_3^{\gamma Z}}{F_1^{\gamma}}\right]$$

$$Y_1 = \frac{1+(1-y)^2 - y^2(1-r^2/(1+R^{\gamma Z})) - xyM/E}{1+(1-y)^2 - y^2(1-r^2/(1+R^{\gamma})) - xyM/E}\left(\frac{1+R^{\gamma Z}}{1+R^{\gamma}}\right) \neq 1$$

higher twist, TMCs, …, enter structure functions, break Callan-Gross: $R^{\gamma} \neq R^{\gamma Z} \neq 0$

$\rightarrow$ JLab20 kinematic range would extend lever arm to control $\sim 1/Q^2$

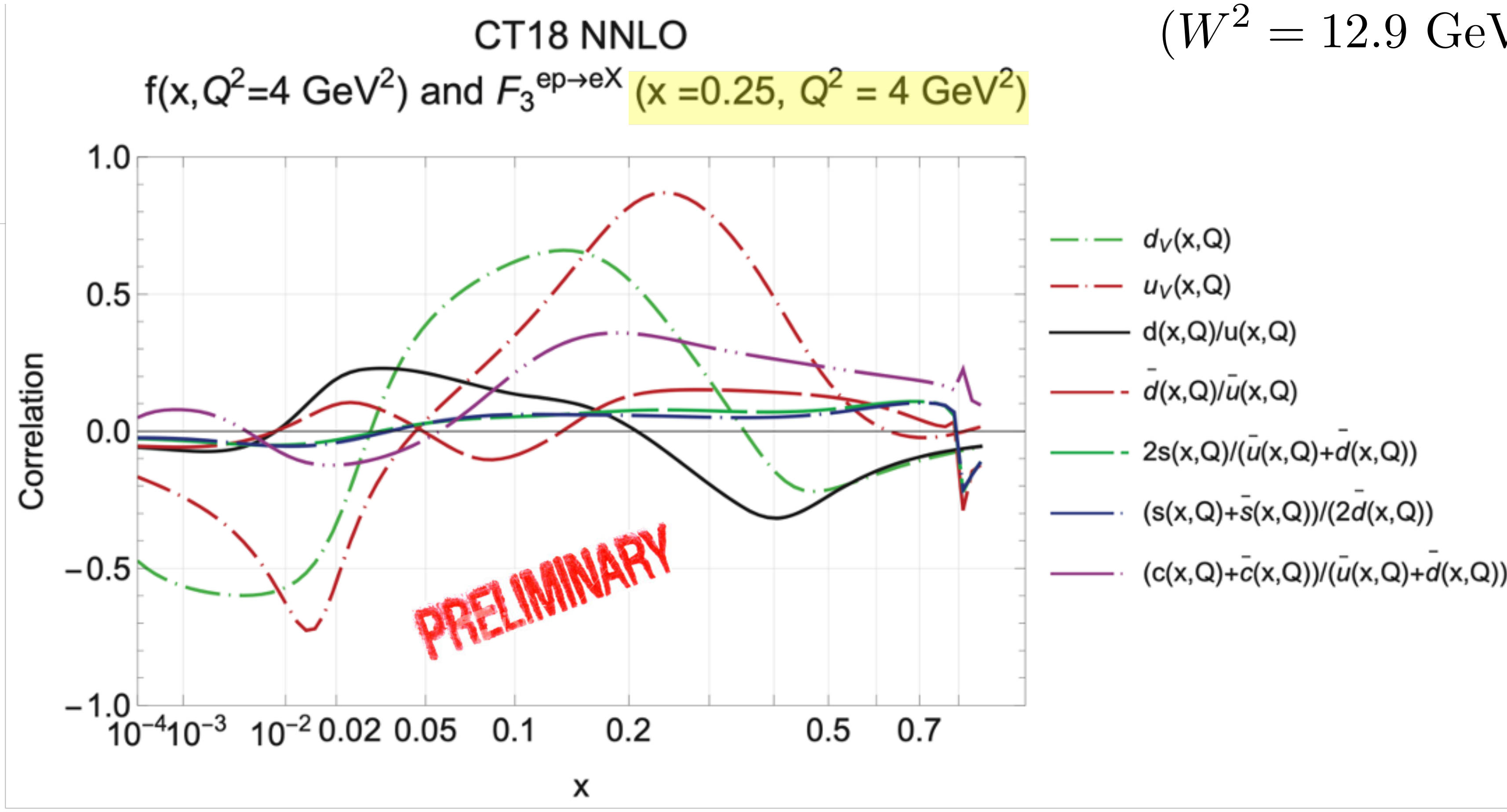

$(W^2 = 12.9 \text{ GeV}^2)$

realistic APV PDF impact studies will require careful understanding of systematics

→ as a proxy, consider PDF correlations with $F_3^{\gamma Z} \sim q - \bar{q}$

post-CT18 fit, lattice constraints to $s \neq \bar{s}$

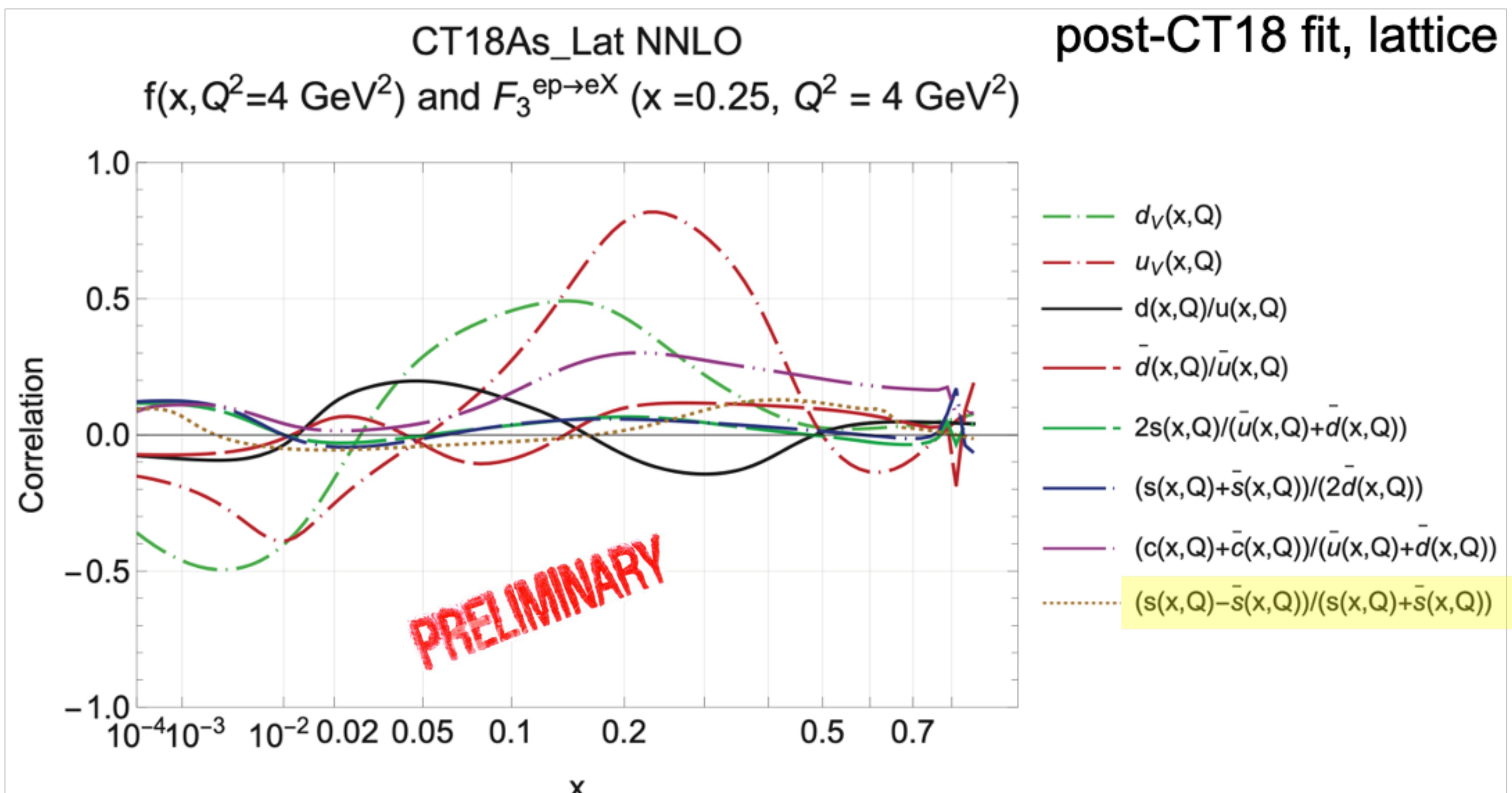

NEW:
CT18 NNLO correlations with $F_3^{\gamma Z}$

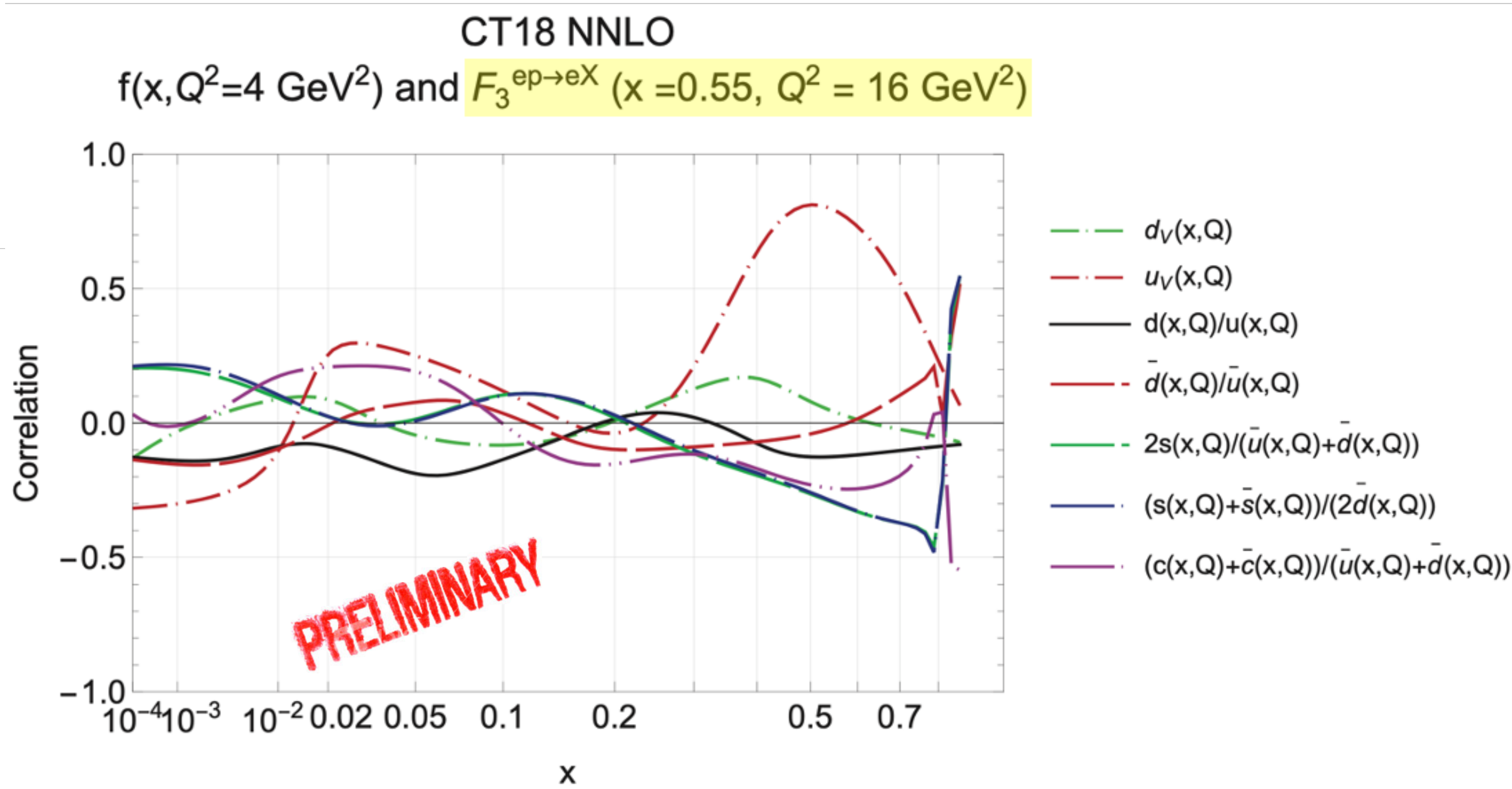

→ PDF correlations have sharp dependence on sampled x, Q^2

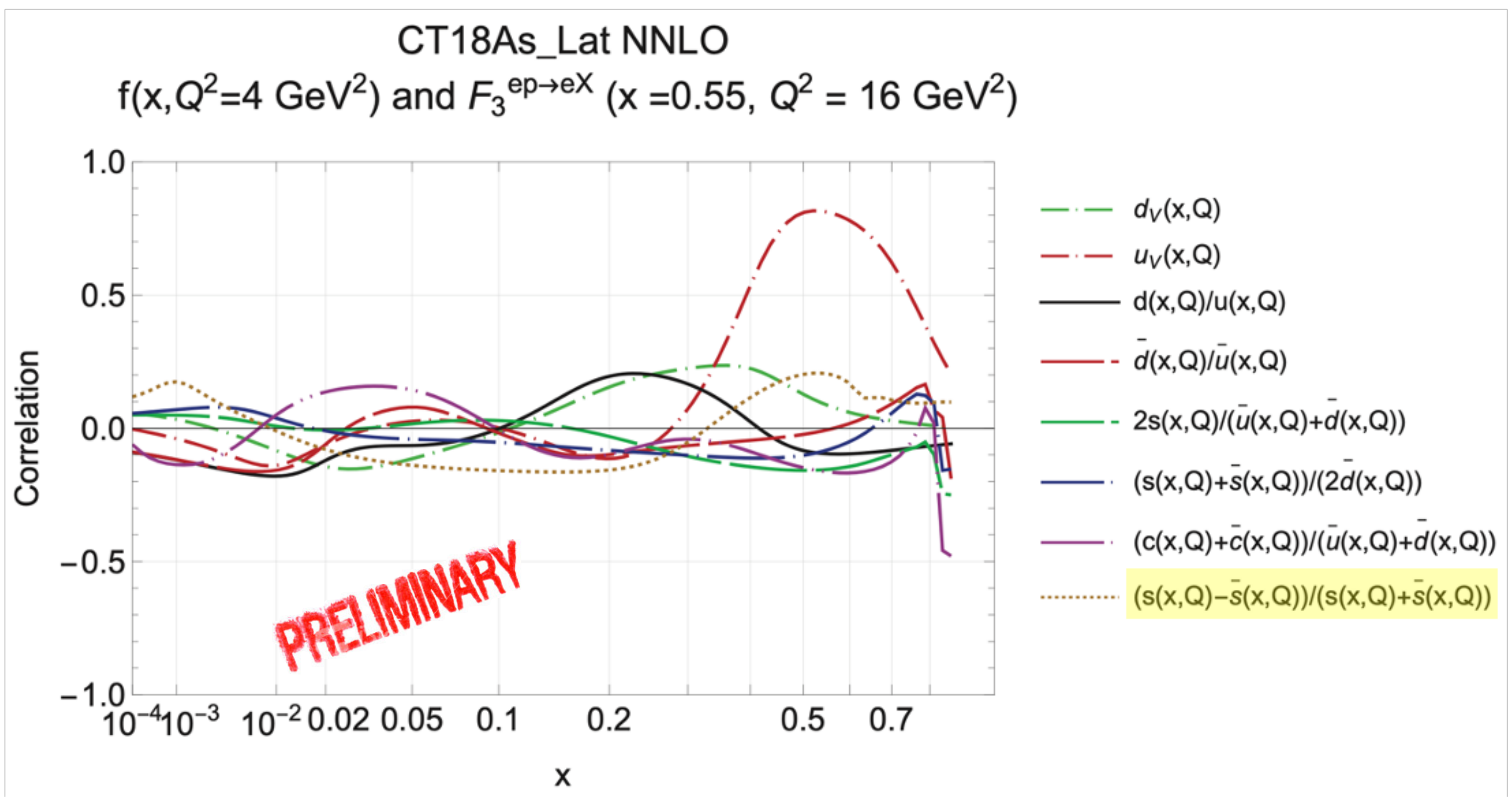

→ PDF correlations suggest strong potential sensitivity to high-x valence-like combinations

NEW:
CT18 NNLO correlations with $F_3^{\gamma Z}$

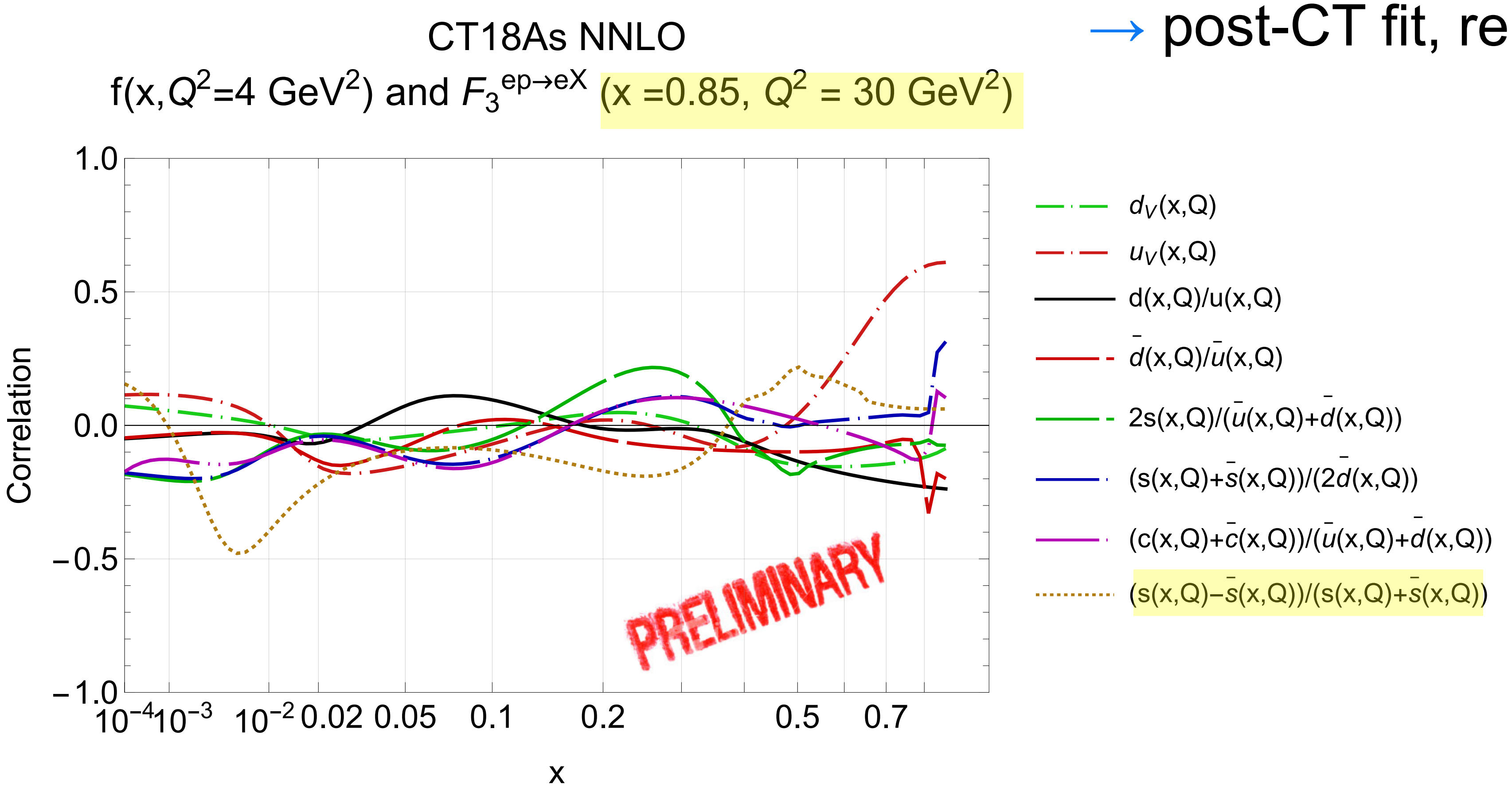

→ post-CT fit, releases $s = \bar{s}$

→ PDF correlations suggest strong potential sensitivity to high-x valence-like combinations

→ role of $s - \bar{s}$ in some kinematical regions (will require further impact studies)

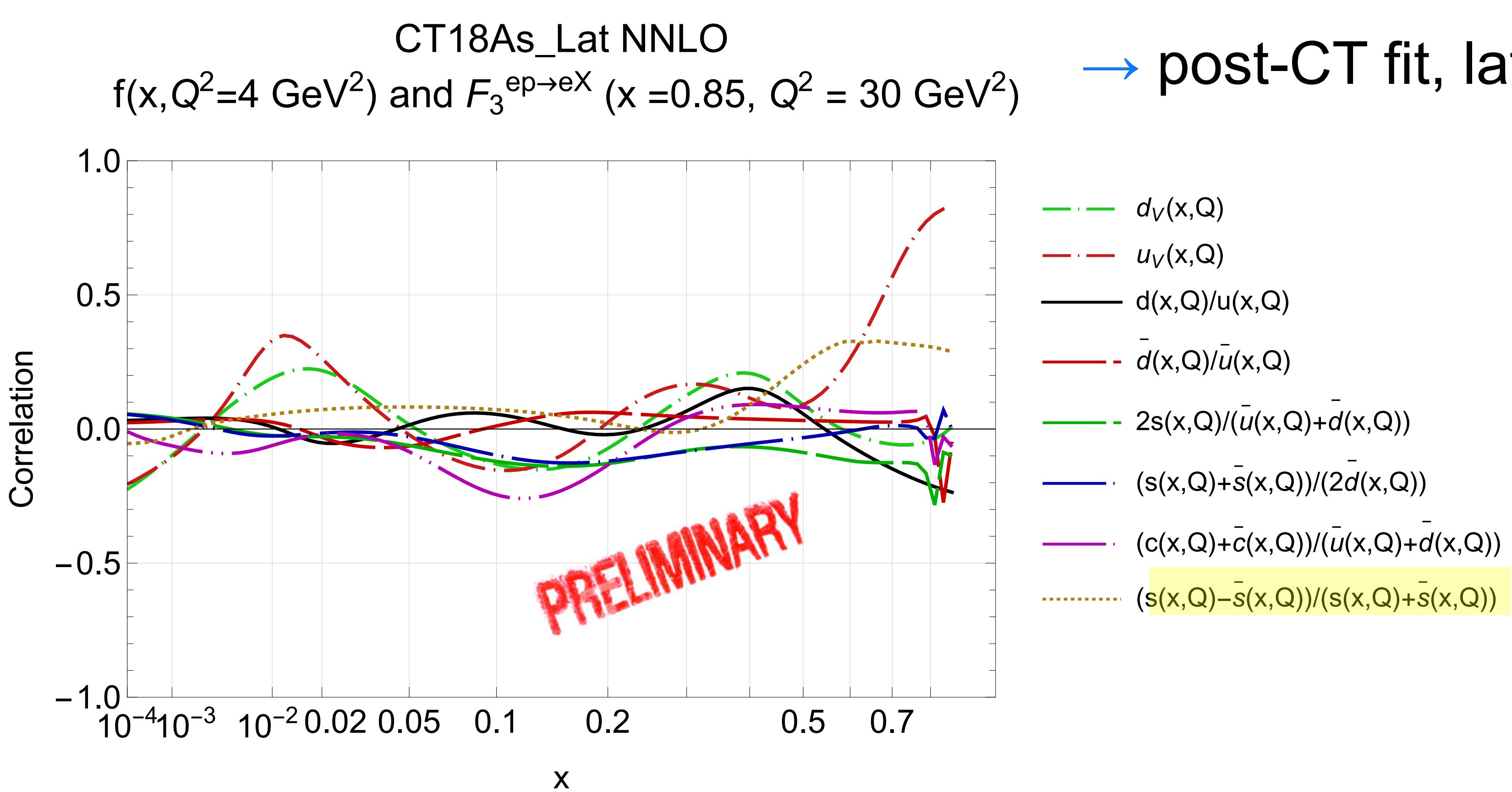

→ post-CT fit, lattice constrains $s \neq \bar{s}$

While $F_3^{\gamma Z}$ has sensitivity to $q - \bar{q}$ combinations, identifying a nonzero $c - \bar{c}$ will be very challenging.

NEW:
CT18 NNLO correlations with $F_3^{\gamma Z}$

Conclusions

CTEQ-TEA proposal to improve flavor separation in the sea with JLab at 22 GeV:

I. predict large-x PDFs at a low-Q energy using data at high x, such as LHC forward-backward asymmetry in Drell-Yan pair production.

II. systematic tools to predict NNLO PDFs at low Q^2, *i.e.*, to separate higher twists.

III. predictions for hadron structure part of APV.

The CTEQ-TEA has systematically studied related corrections, e.g., large x and deuteron, and will be able to provide a baseline leading-power PDF ensemble for low Q^2 kinematics.

BACKUP SLIDES

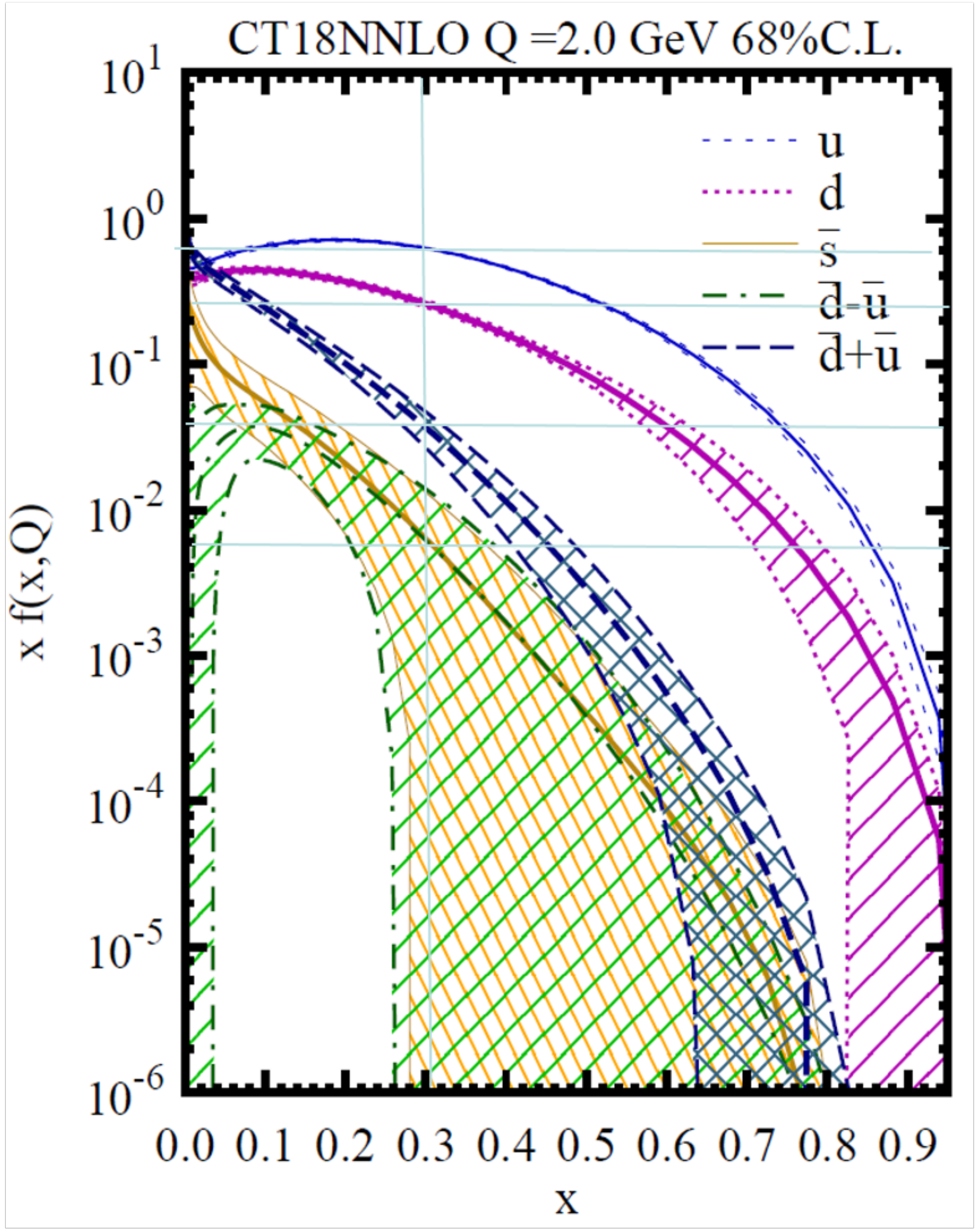

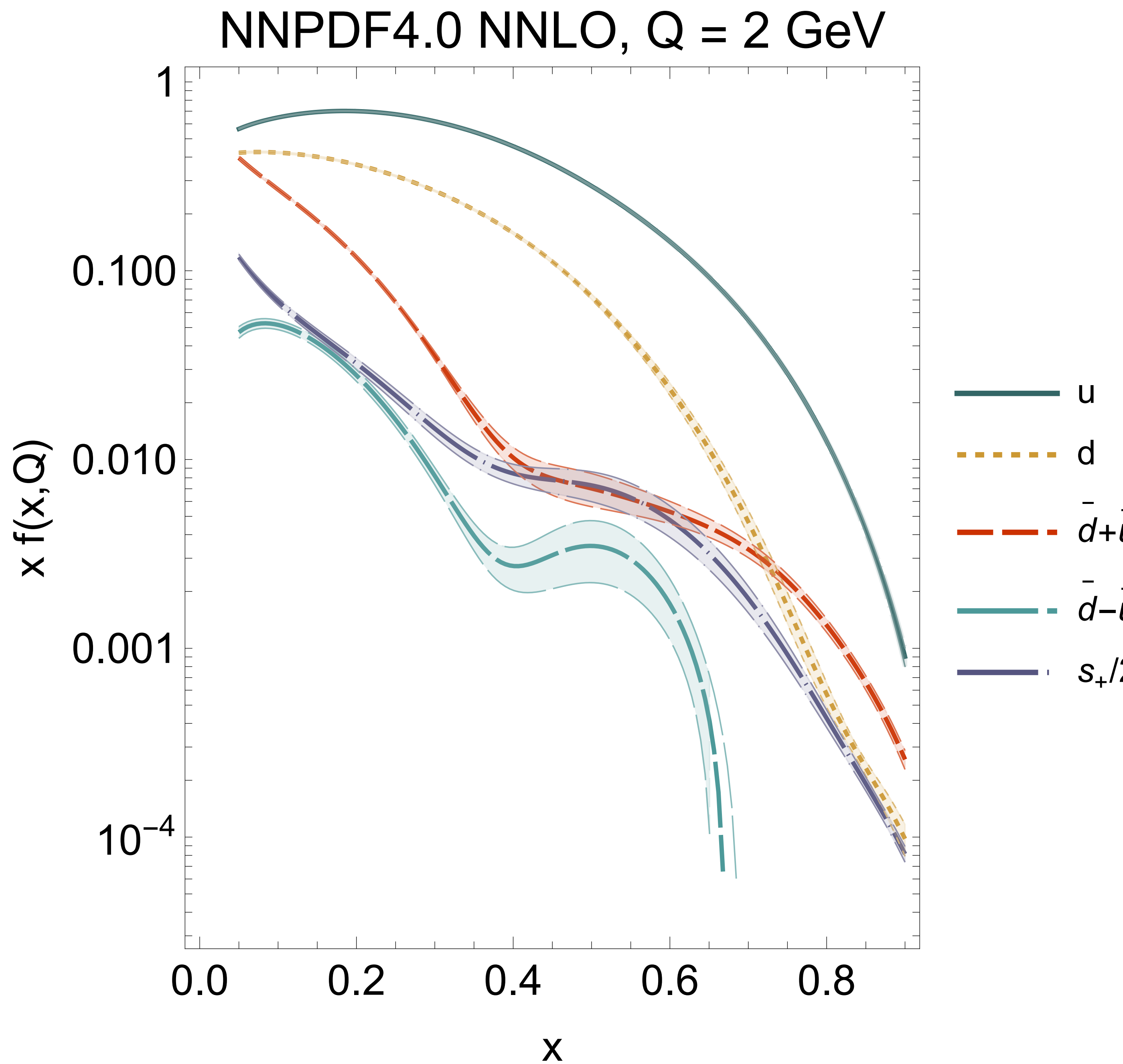

Low-sea scenario with smooth light-sea quarks. Larger PDF uncertainties reflect representative sampling of PDF solutions [2205.10444, accepted to PRD.]

High-sea scenario with non-smooth light-sea quarks, with sea PDFs that can be larger than valence PDFs at large x.

FC PDF moments as F.o.M.

even restrictive uncertainties give moments consistent with zero

→ broaden further for default CT tol.

→ lattice may give $\langle x \rangle_{c^+}$, $\langle x^2 \rangle_{c^-}$

$$\langle x \rangle_{\rm FC} \equiv \langle x \rangle_{c^+}[Q_0 = 1.27\,\mathrm{GeV}]$$

$$= 0.0048\,{}^{+0.0063}_{-0.0043}\,\left({}^{+0.0090}_{-0.0048}\right),\ \mathrm{CT18\ (BHPS3)}$$

$$= 0.0041\,{}^{+0.0049}_{-0.0041}\,\left({}^{+0.0091}_{-0.0041}\right),\ \mathrm{CT18X\ (BHPS3)}$$

$$= 0.0057\,{}^{+0.0048}_{-0.0045}\,\left({}^{+0.0084}_{-0.0057}\right),\ \mathrm{CT18\ (MBMC)}$$

$$= 0.0061\,{}^{+0.0030}_{-0.0038}\,\left({}^{+0.0064}_{-0.0061}\right),\ \mathrm{CT18\ (MBME)}$$

$\Delta\chi^2 \leq 10$ (restrictive tolerance)

$\Delta\chi^2 \leq 30$ (~CT standard tolerance)

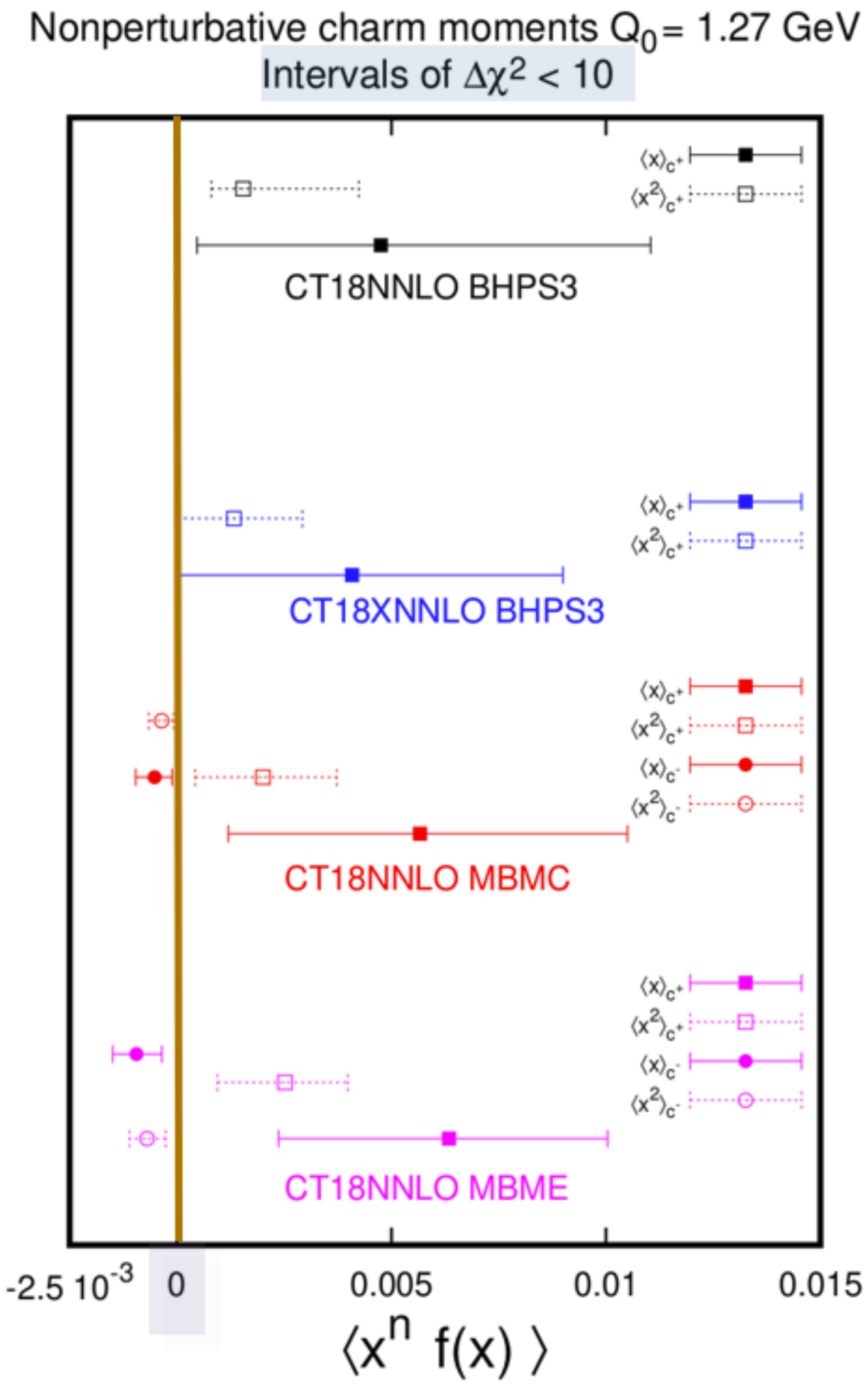

potential connection to nonperturbative charm?

pQCD only very weakly breaks $c = \bar{c}$ through HO corrections

→ large(r) charm asymmetry would signal nonpert dynamics, IC

→ MBM breaks $c = \bar{c}$ through hadronic interactions

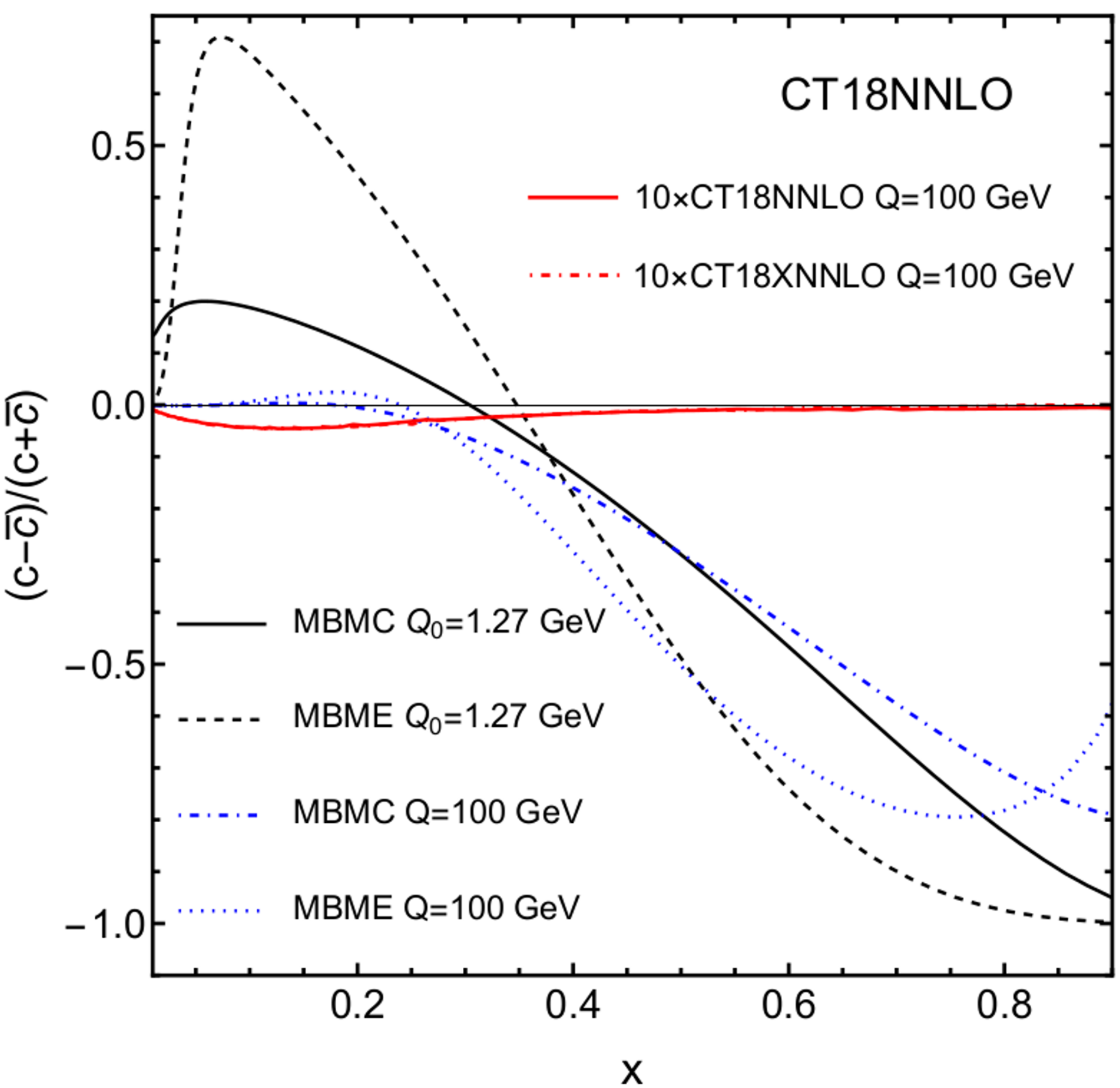

consider two MBM models as ***examples*** (<u>not predictions</u>)

→ asymmetry small but ratio (left) can be bigger; **hard to extract from data**

→ hypothetically, very precise APV could constrain/test charm asymmetry; constraints to corresponding strange asymmetry could indirectly help as well

nonperturbative QCD can generate a low-scale charm PDF

Fock expansion

Brodsky, Hoyer, Peterson, Sakai (**BHPS**); Phys. Lett. **B93** (1980) 451.

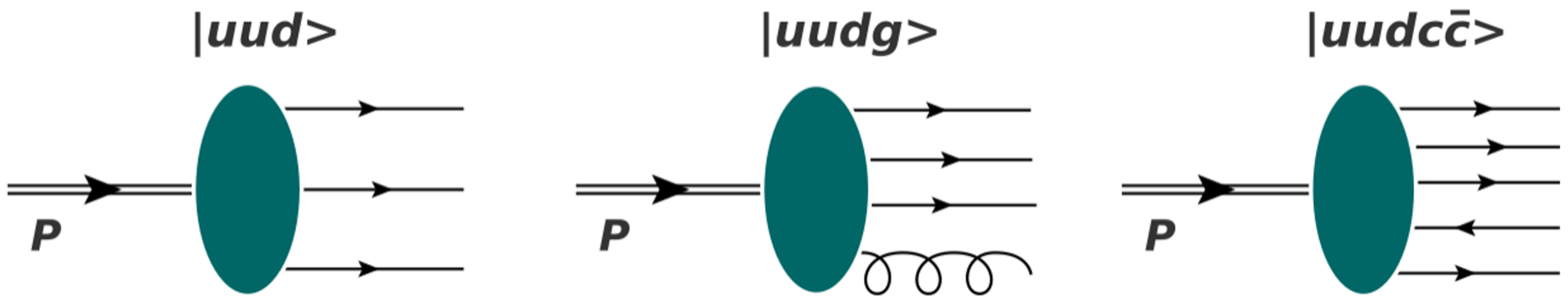

IC PDF: transition matrix element, $|\text{proton}\rangle \to |uudc\bar{c}\rangle$

$$P(p \to uudc\bar{c}) \sim \left[M^2 - \sum_{i=1}^{5} \frac{k_{\perp i}^2 + m_i^2}{x_i} \right]^{-2}$$

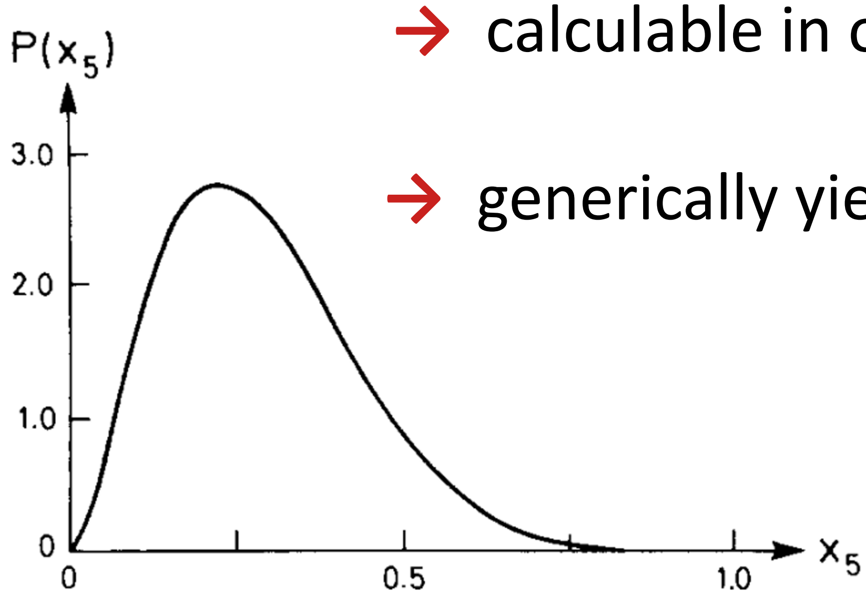

→ calculable in old-fashioned perturbation theory; **scalar** field theory

→ generically yields valence-like shape; governed by charm masses

$$m_c = m_{\bar{c}} \implies c^{\mathrm{BHPS}}(x) = \bar{c}^{\mathrm{BHPS}}(x)$$

alternative but similar representations exist

Blumlein; Phys. Lett. **B753** (2016) 619.

IC models and **formal QCD**

models simulate nucleon wave function; aim to *mimic* nonpert QCD

- → bound-state structure driven by constituent-quark masses
- → integrate away gluonic degrees-of-freedom
- → connect to SU(4) flavor-symm breaking (in meson-baryon models [MBMs])

<u>BUT</u>: IC models in systematically-improvable QCD calculations unclear

- → based on *truncated* Fock-state or similar wave function expansions
- → no obvious mapping onto factorization theorems
- → ambiguity regarding fact. scale, μ, in IC models

$$F(x,Q) = \sum_{a=0}^{N_f} \int_x^1 \frac{d\xi}{\xi}\, \mathcal{C}_a\left(\frac{x}{\xi}, \frac{Q}{\mu}, \frac{m_c}{\mu}; \alpha_s(\mu)\right) f_{a/p}(\xi,\mu) + \mathcal{O}(\Lambda^2/m_c^2, \Lambda^2/Q^2)$$

PDF analyses extract <u>fitted charm</u> (FC) ≠ intrinsic charm (IC)

Unusual unsmooth $\bar{d}/\bar{u}$ at large x

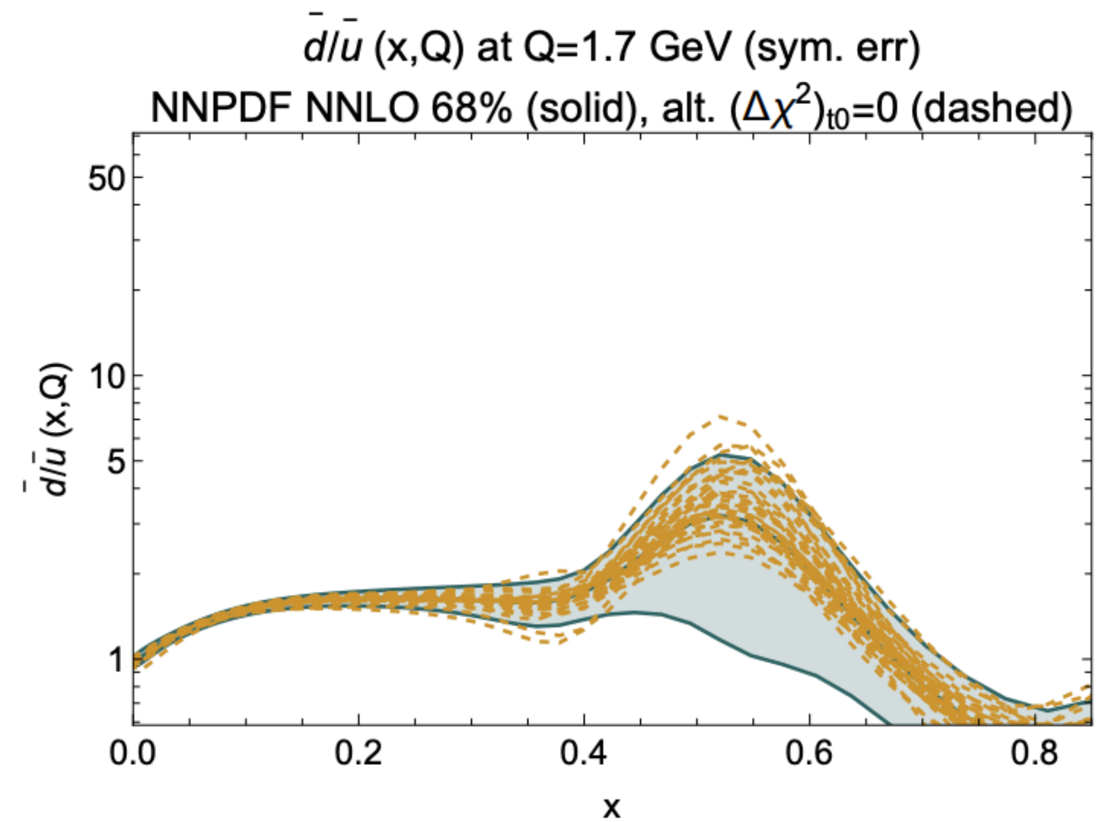

Hopscotch uncertainties wash out reported evidence for large positive strangeness asymmetry and non-zero intrinsic charm.

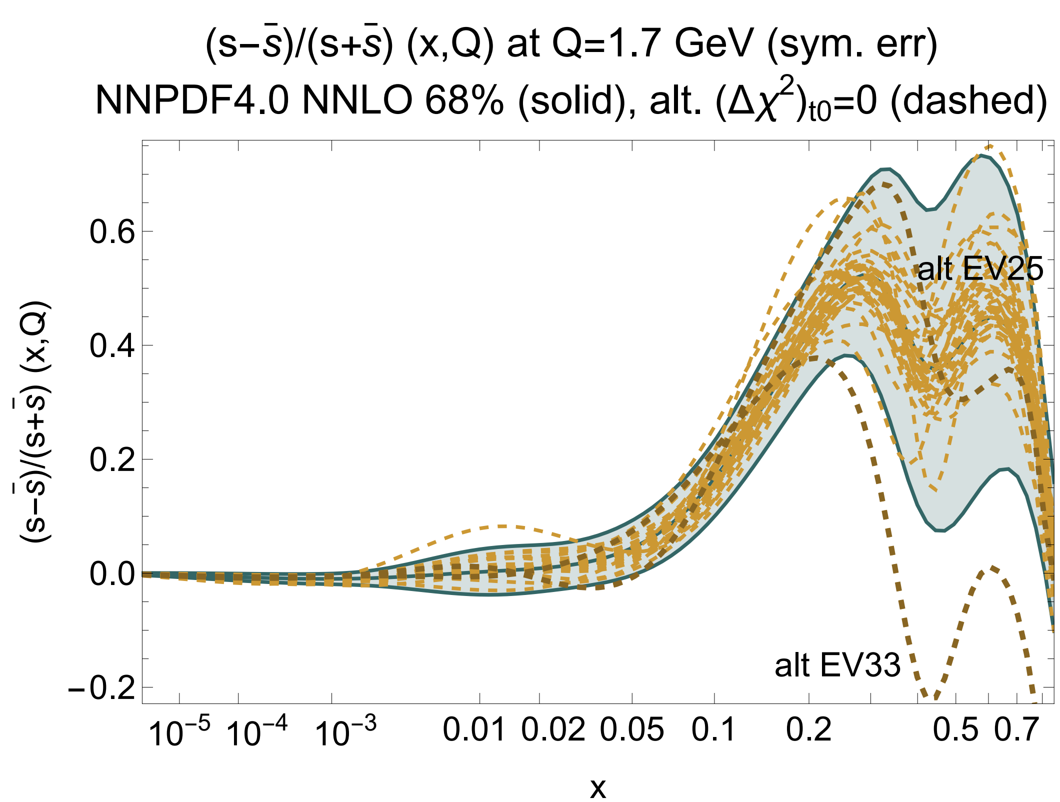

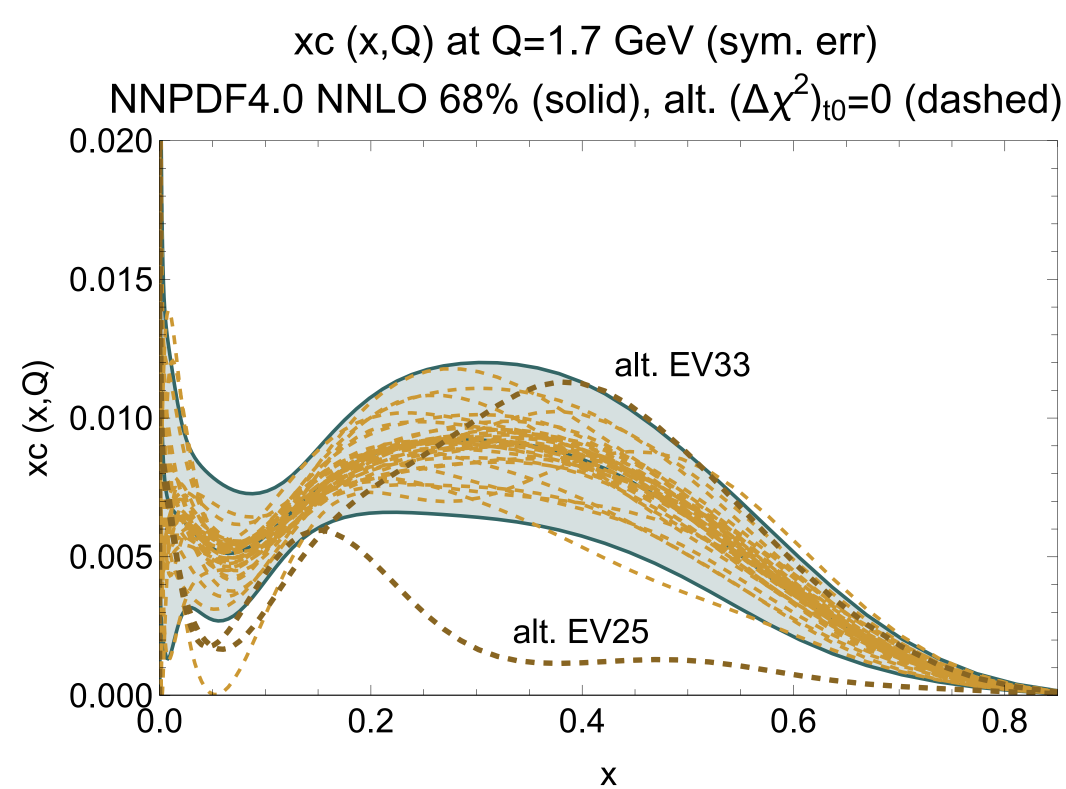

possibilities with parity violation

lepton beam (parity-violating) helicity asymmetries, APV, combine sensitivity to electroweak couplings (& possible TeV-scale anomalies), proton structure functions:

$$A^{\mathrm{PV}} = \frac{\sigma_R - \sigma_L}{\sigma_R + \sigma_L}$$

$\rightarrow$ right-left asymmetry can be expanded,

$$A^{\mathrm{PV}} = -\left(\frac{G_F Q^2}{4\sqrt{2}\pi\alpha}\right)\left[g_A^e \; Y_1 \; \frac{F_1^{\gamma Z}}{F_1^{\gamma}} \; + \; \frac{g_V^e}{2} \; Y_3 \; \frac{F_3^{\gamma Z}}{F_1^{\gamma}}\right]$$

$\rightarrow$ with sufficient control over EW theory, may help unravel PDF flavor dep,

$$F_1^{\gamma Z}(x) = \sum_q e_q \; g_V^q \; \left(q(x) + \bar{q}(x)\right)$$

$$F_3^{\gamma Z}(x) = 2\sum_q e_q \; g_A^q \; \left(q(x) - \bar{q}(x)\right)$$

NB: these are *leading-order* expns; full PDF impact of APV requires careful study

Forward-backward asymmetry at $Q = 1\text{TeV}$

NEW:
based on predictions from Fu, Hou, Yuan, et al.

Drell-Yan backward-forward dilepton production is sensitive to light sea and gluon for increasing M_{ll}.

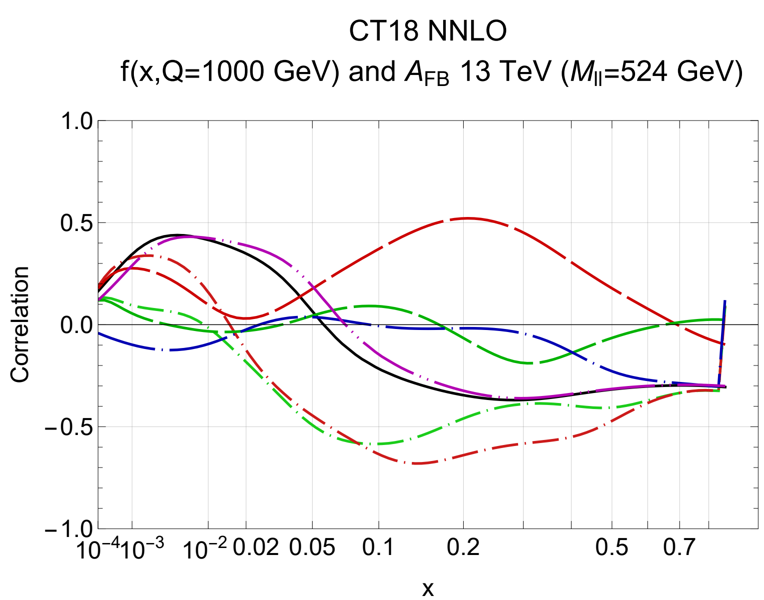

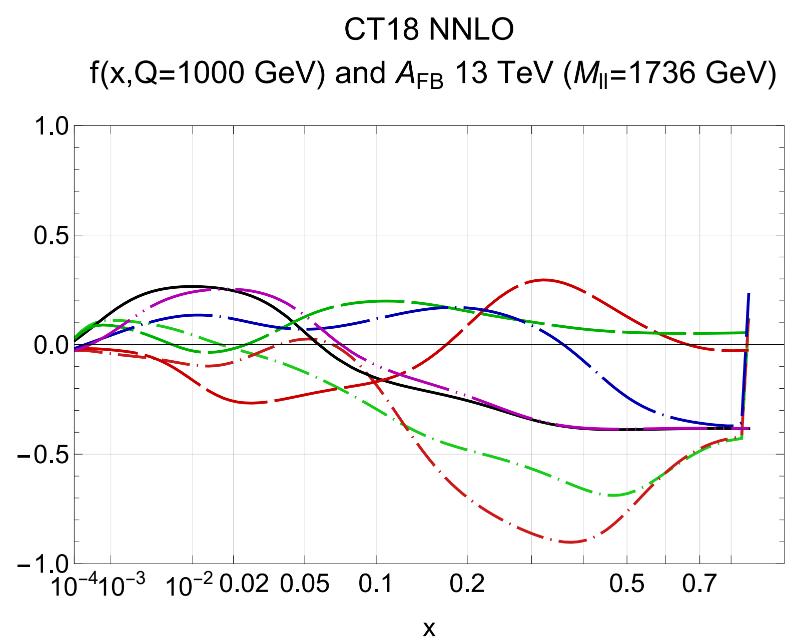

Strong anti-correlation of AFB with $\bar{u}$ and $\bar{d}$ (and gluon) at large x for increasing M_{ll}.

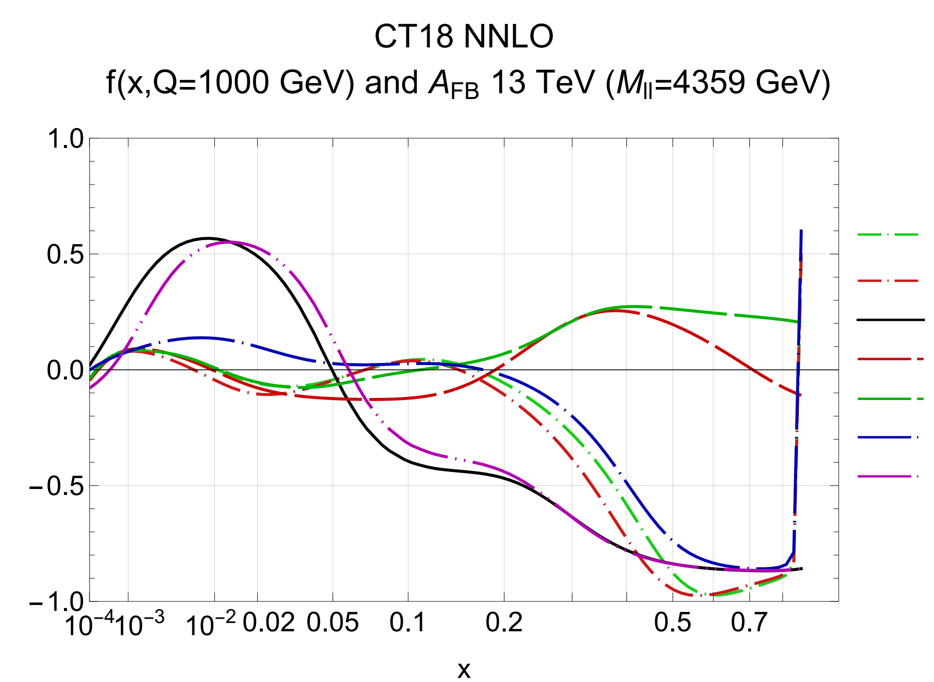

PRELIMINARY

Growing correlation of AFB with gluon at $x < 0.2$.

see also [Ball et al, EPJC 2022 82]

A fast test of experimental constraints using L_2 sensitivity

T.J. Hobbs et al., 1904.00022

- Requires:
  - Hessian or Monte Carlo error PDFs
  - χ^2 values for fitted or envisioned experiments for each error PDF

- Quantifies:
  - strengths of constraints from individual experiments on given PDFs
  - agreement among the experiments (universality of the best-fit PDFs)
  - sensitivity of processes not included in the global fit

If data point residuals for each error PDF set are also provided, a related $\boldsymbol{L_1}$ **sensitivity** (B. T. Wang et al., 1803.02777, see backup) can be computed to visualize kinematic distributions of experimental constraints in the x-Q plane

Tolerance hypersphere in the PDF space

2-dim (i,j) rendition of N-dim (26) PDF parameter space

Hessian method: Pumplin et al., 2001

A symmetric PDF error for a physical observable X is given by

$$\Delta X = \vec{\nabla} X \cdot \vec{z}_m = \left|\vec{\nabla} X\right|$$
$$= \frac{1}{2}\sqrt{\sum_{i=1}^{N}\left(X_i^{(+)} - X_i^{(-)}\right)^2}$$

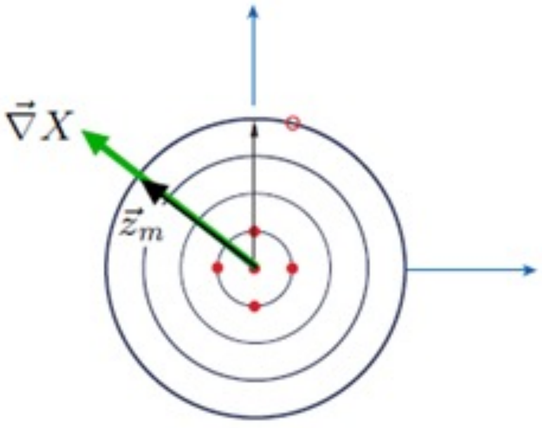

(b)
Orthonormal eigenvector basis

Correlation cosine for observables X and Y:

hep-ph/0110378

$$\cos\varphi = \frac{\vec{\nabla} X \cdot \vec{\nabla} Y}{\Delta X \Delta Y} =$$
$$\frac{1}{4\Delta X\,\Delta Y}\sum_{i=1}^{N}\left(X_i^{(+)} - X_i^{(-)}\right)\left(Y_i^{(+)} - Y_i^{(-)}\right)$$

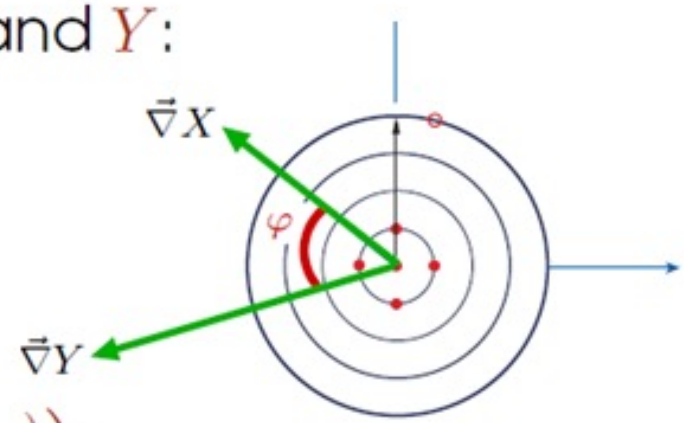

(b)
Orthonormal eigenvector basis

L_2 sensitivity, definition

$S_{f,L_2}(E)$ for experiment E is the estimated $\Delta\chi^2_E$ for this experiment when a PDF $f_a(x_i, Q_i)$ increases by the +68% c.l. Hessian PDF uncertainty

Take $X = f_a(x_i, Q_i)$ or $\sigma(f)$; $Y = \chi^2_E$ for experiment E.

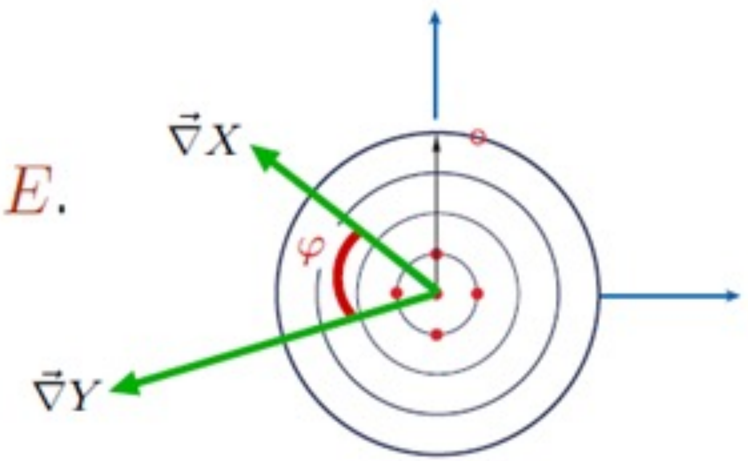

$$S_{f,L_2} \equiv \Delta Y(\vec{z}_{m,X}) = \vec{\nabla}Y \cdot \vec{z}_{m,X} = \vec{\nabla}Y \cdot \frac{\vec{\nabla X}}{|\vec{\nabla X}|} = \Delta Y \cos\varphi.$$

A fast version of the Lagrange Multiplier scan of χ^2_E along the direction of $f_a(x_i, Q_i)$!

IV. Towards a thorough understanding of uncertainties in global analyses

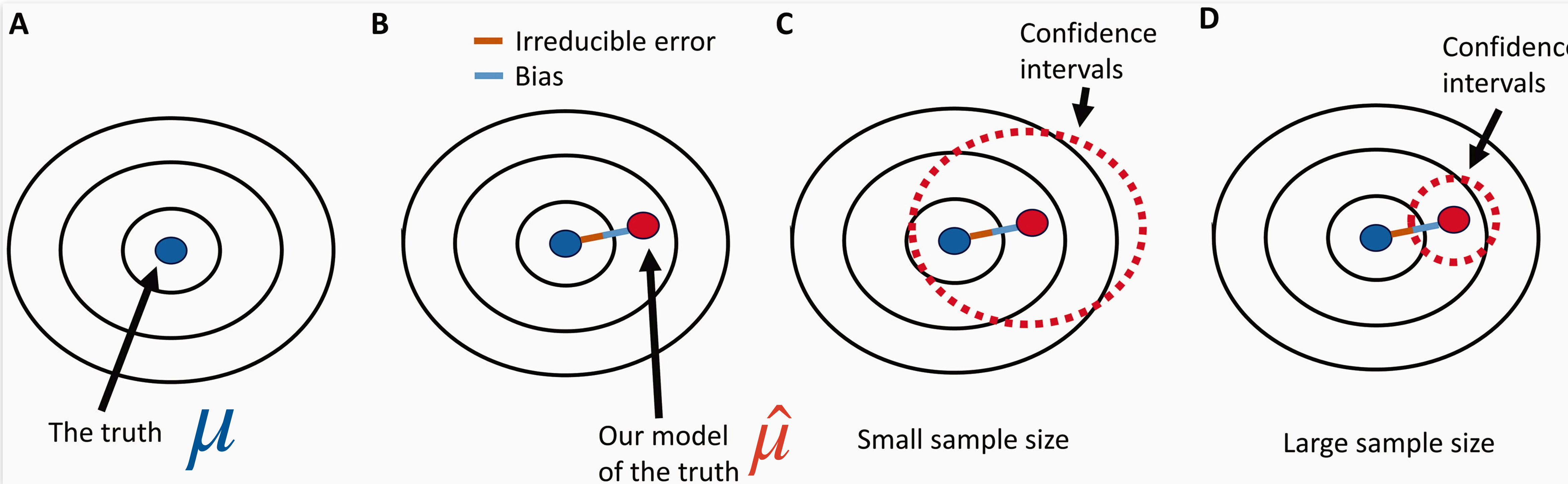

Pavlos Msaouel (2022)
Cancer Investigation, 40:7, 567-576

With an increasing size of sample $n \to \infty$, under a set of hypotheses, it is usually expected that the *deviation* on an observable decreases like $\left(\sqrt{n}\right)^{-1}$.

That's the law of large numbers.

What uncertainties keep us from including *the truth*, μ?

The law of large numbers disregards the *quality of the sampling*, 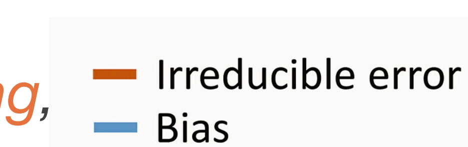

.

Xiao-Li Meng
The Annals of Applied Statistics
Vol. 12 (2018), p. 685

Trio identity

Xiao-Li Meng
The Annals of Applied Statistics
Vol. 12 (2018), p. 685

$$\boxed{\mu - \hat{\mu} = \text{(data+sampling defect)} \times \text{(measure discrepancy)} \times \text{(inherent problem difficulty)}}$$

depends on the sampling algorithm

can tend to $\left(\sqrt{n}\right)^{-1}$ for random sampling

Irreducible error
Bias

$\equiv$ statistical model, quality of data,…

Large sample size

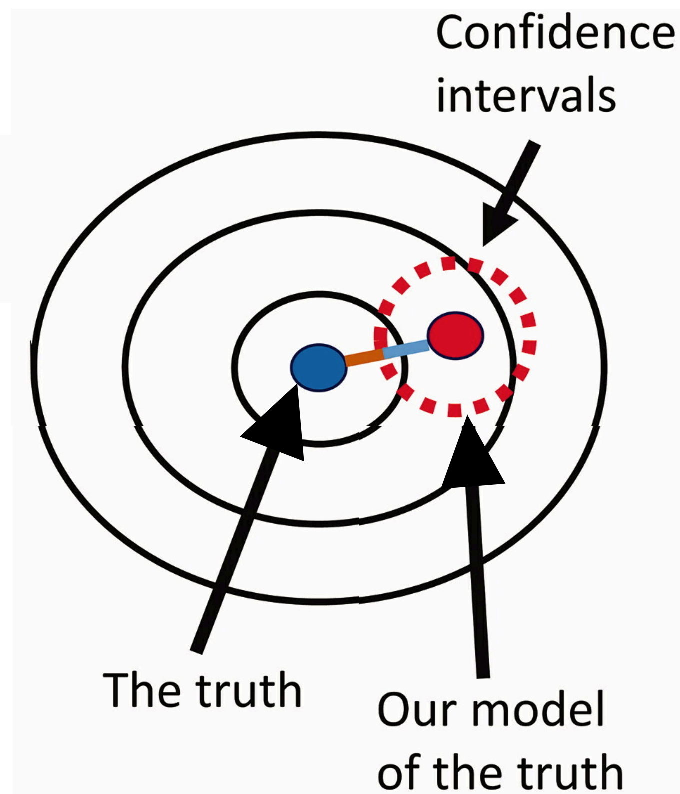

For a sample of n items from the population of size N, we can consider an array built by the random spanning of the binary responses of the $N - n$ (0) and n (1) items, so that

$$\boxed{\mu - \hat{\mu} = \mathrm{Corr}[\text{observable, sampling quality}] \times \sqrt{\frac{N}{n} - 1} \times \sigma(\text{observable})}$$

IV. Towards a thorough understanding of uncertainties in global analyses

*[**AC**, Huston, Nadolsky, Xie, Yan & Yuan, 2205.10444]*
Accepted in PRD

We have devised an algorithm that focuses on the effective dimensions relevant for observables, to challenge Monte Carlo-based analyses. The resulting uncertainty is larger than the nominal one, shown here for (σ_H, σ_Z).

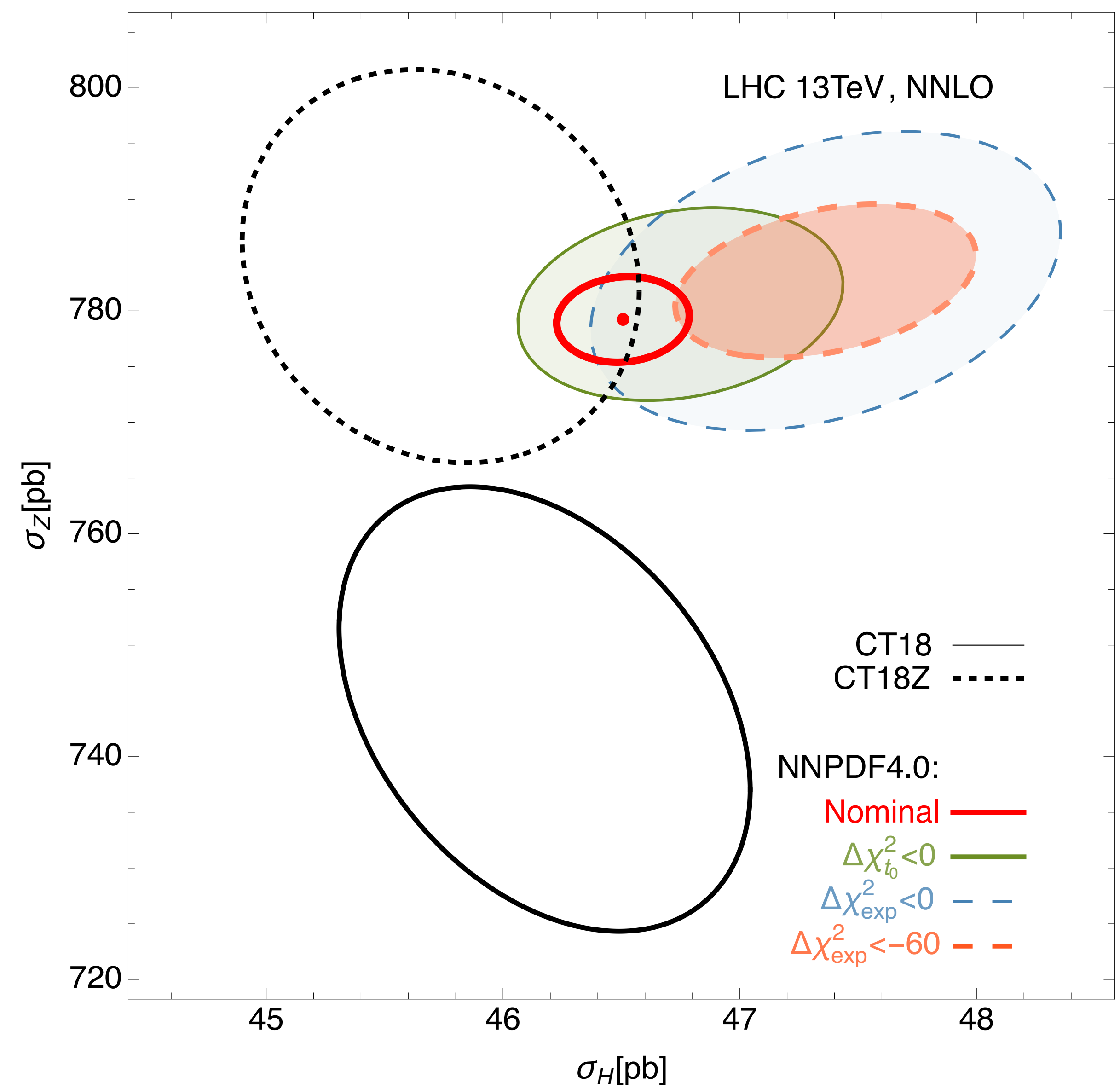

IV. Towards a thorough understanding of uncertainties in global analyses

*[**AC**, Huston, Nadolsky, Xie, Yan & Yuan, 2205.10444]*
Accepted in PRD

We have devised an algorithm that focuses on the effective dimensions relevant for observables, to challenge Monte Carlo-based analyses. The resulting uncertainty is larger than the nominal one, shown here for (σ_H, σ_Z).

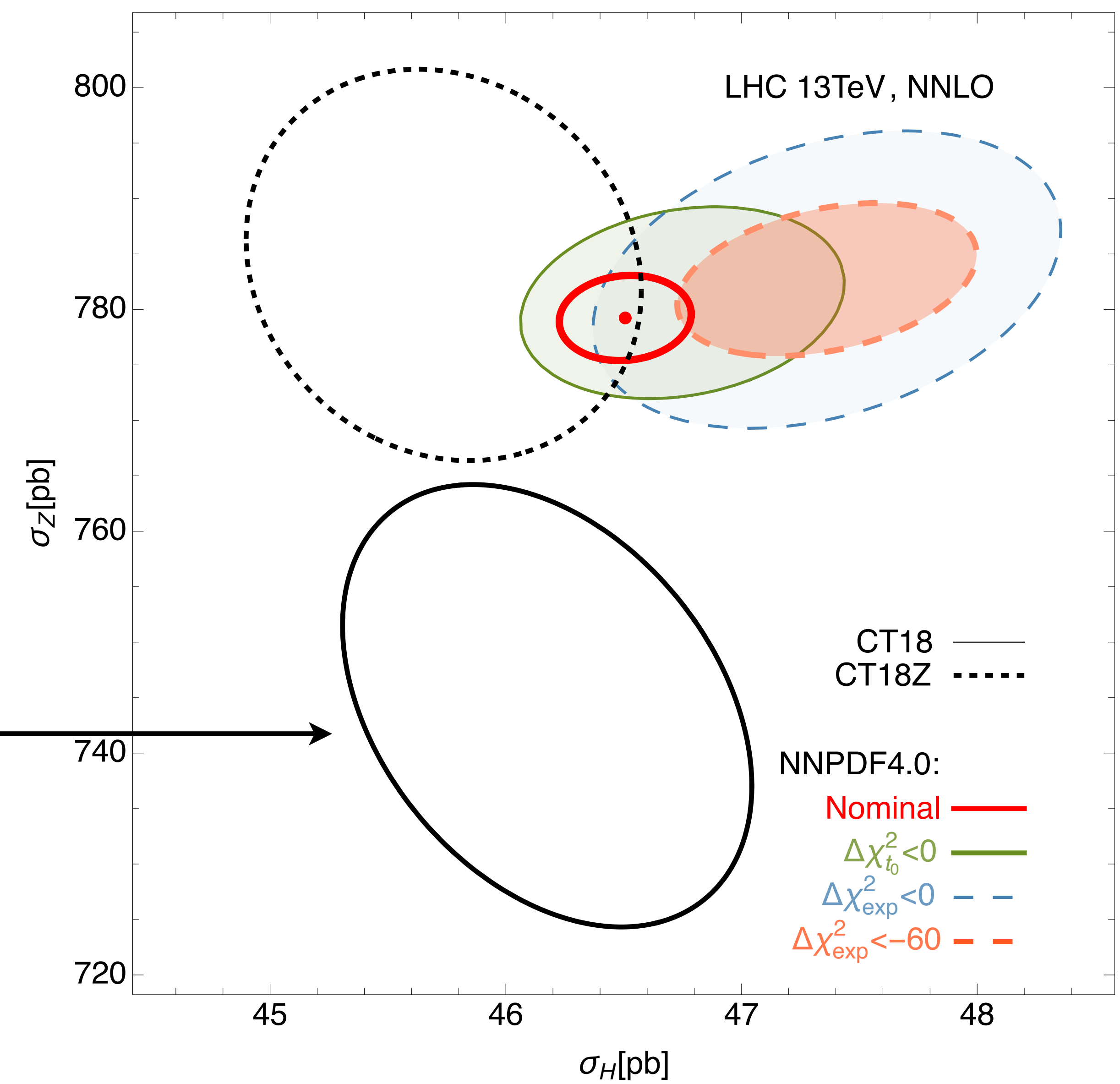

Parton distributions need a representative sampling

*Monte Carlo uncertainties from **sampling bias** found through our dimensional reduction method play a similar role as sampling of parameter space in Hessian uncertainties.*

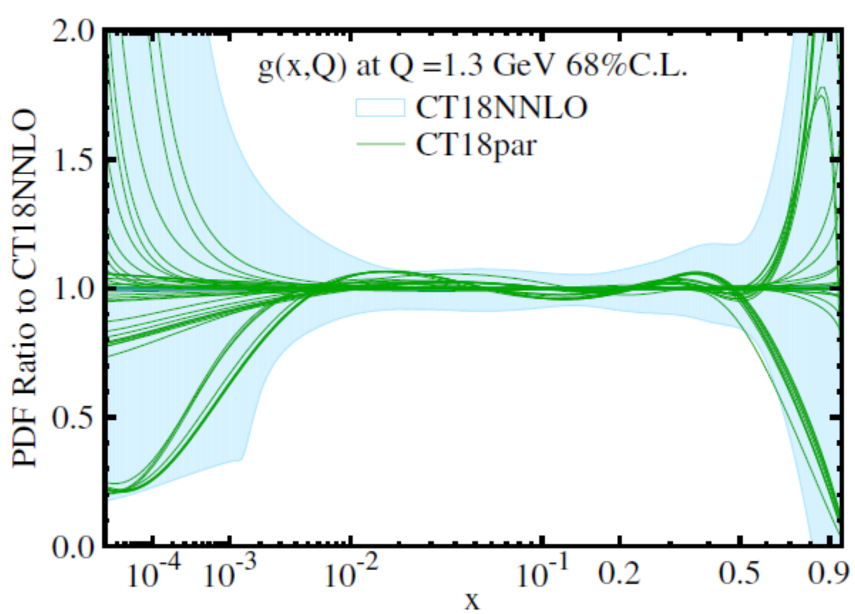

Monte-Carlo sampling sensitivity for PDFs

Regions containing (very) good solutions according to the experimental form of χ^2
(is used in χ^2 summary tables of the NN4.0 article, was a default in the NN4.0 public code)

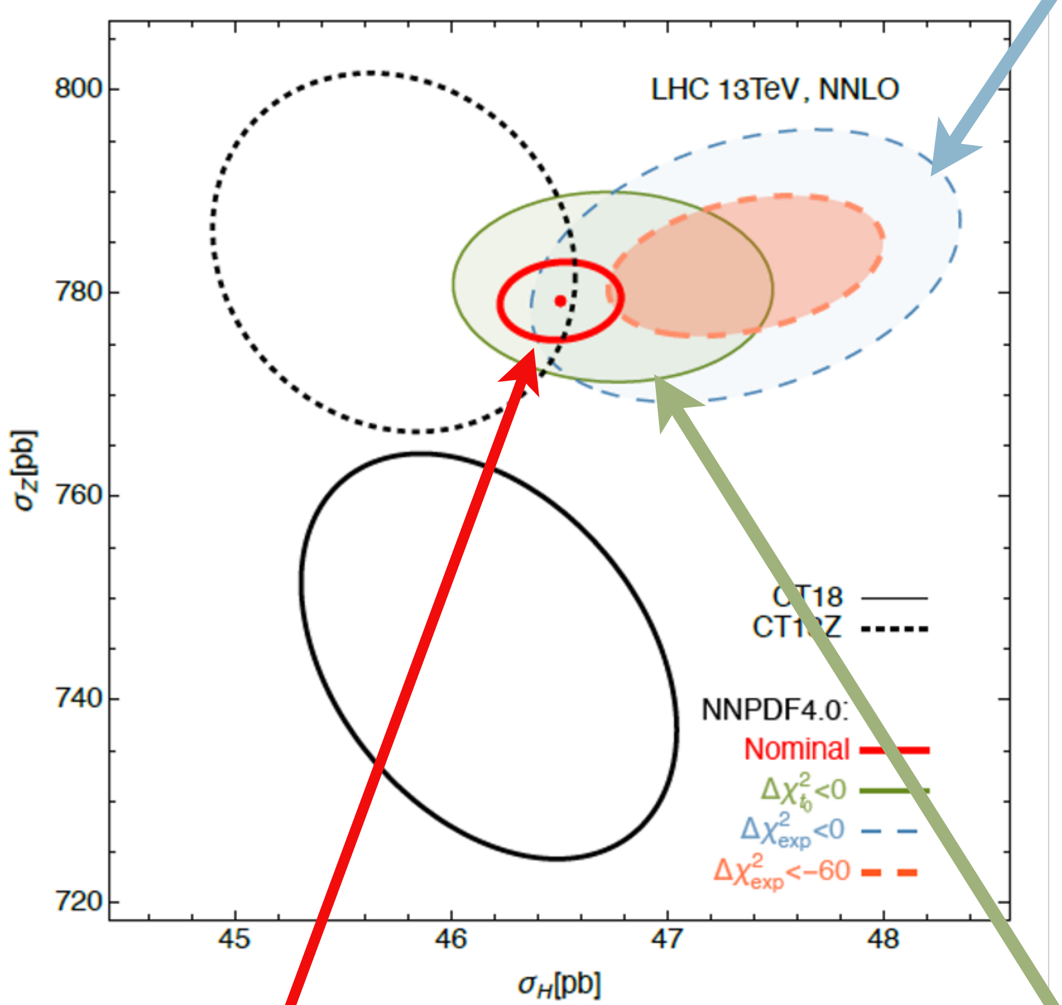

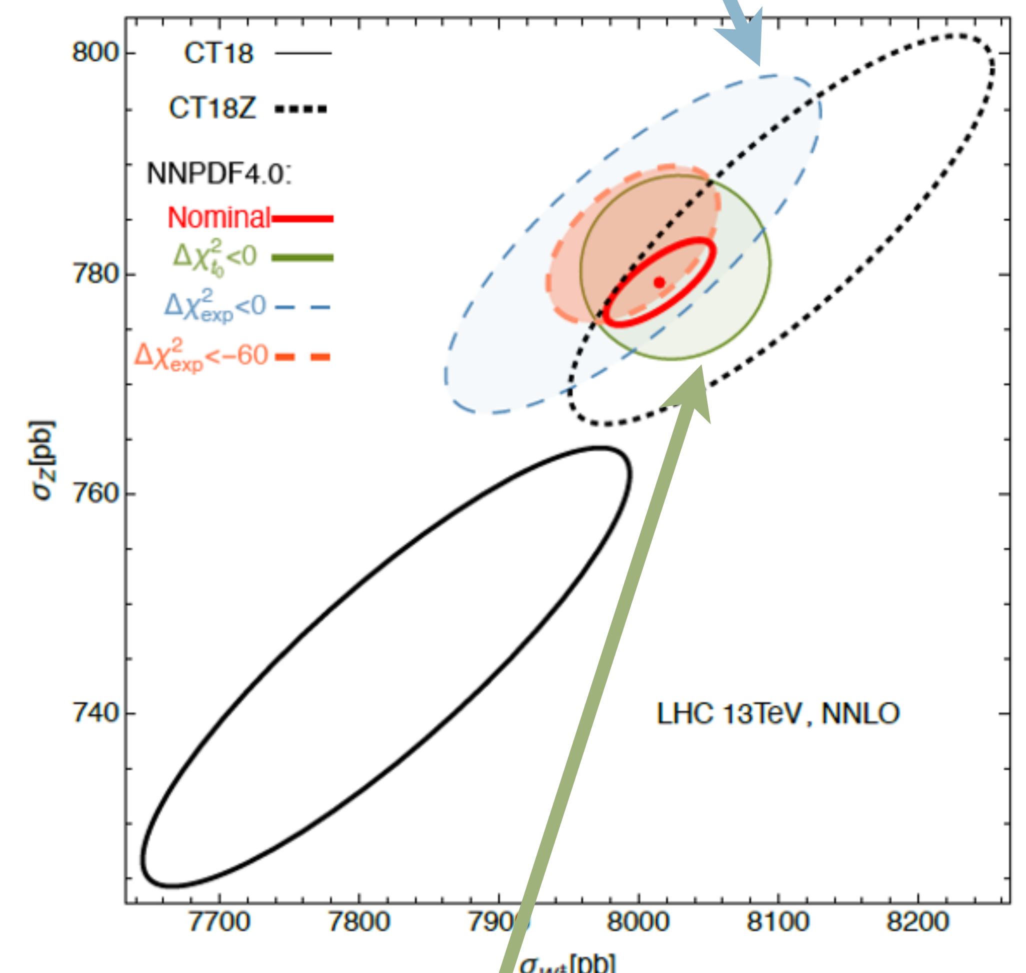

Nominal NN4.0 Hessian or MC 68%cl

Region containing good solutions according to the most recent t_0 form of χ^2
(used to train NN4.0 replicas)

Optimize the inclusion of large-x data

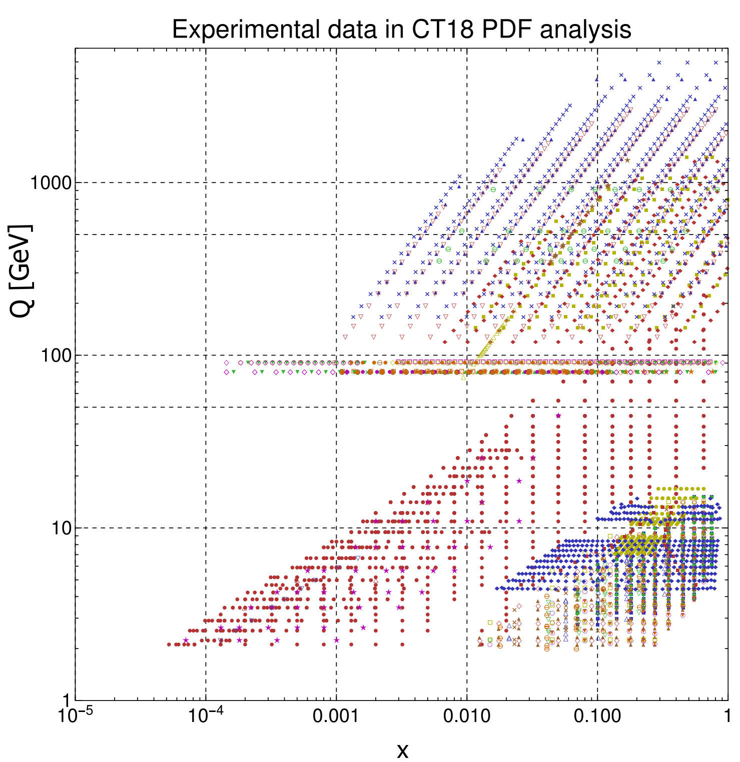

Latest kinematic coverage for CT18

3681 data points from over 39 different experiments

$Q > 2$ GeV and $W^2 > 12.25$ GeV^2

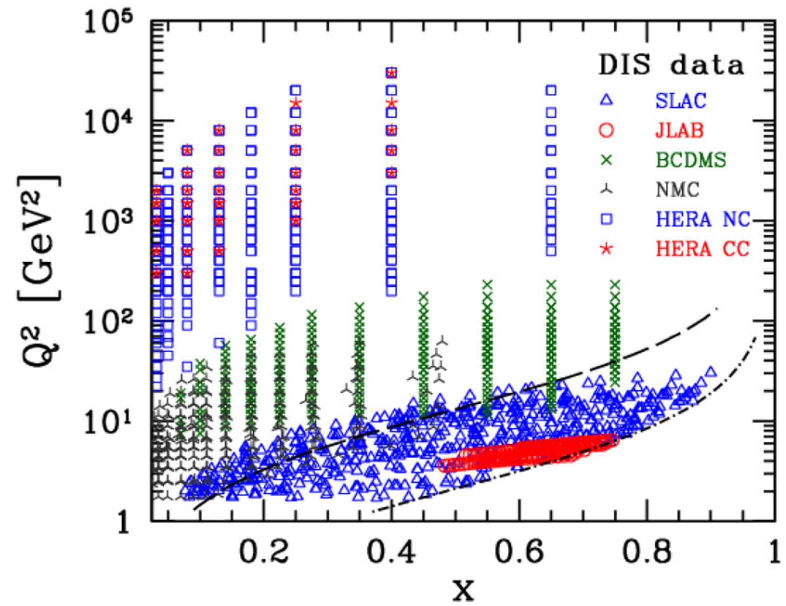

[Owens et al, PRD87]
[Accardi et al, EPJC81]

Old kinematic coverage showing the impact of the W² cuts on data selection

$W^2 > 12.25$ GeV^2 vs $W^2 > 3$ GeV^2

Impact on analysis of the ratio of structure functions nucleon-deuteron

CT18: [Hou et al., PRD103]
CJ15: [Accardi et al., PRD93]

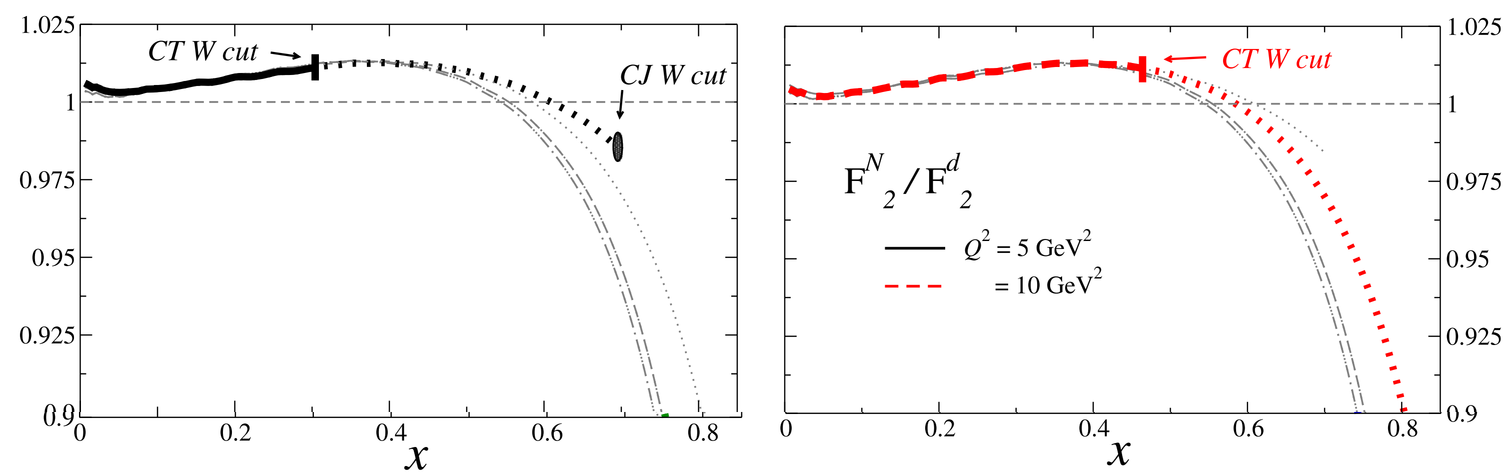

[Accardi et al, EPJC81]

Pheno PDFs with different perspectives

Comparison of CTEQ-TEA (CT) and CTEQ-JLab (CJ) analyses

Sensitivity of PDF configuration with objective function will vary, from data set to data set, between CJ and CT. Importance of deuteron corrections and set of approximations.

[Accardi et al., PRD93]

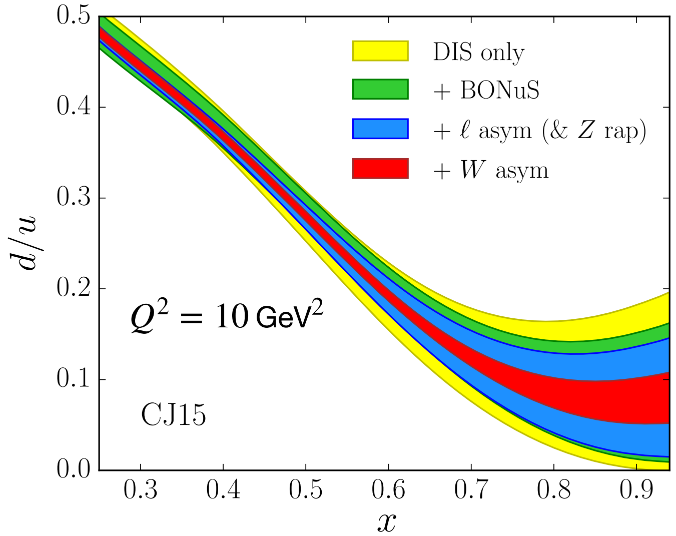

A. Accardi— CJ (04/09 D09)

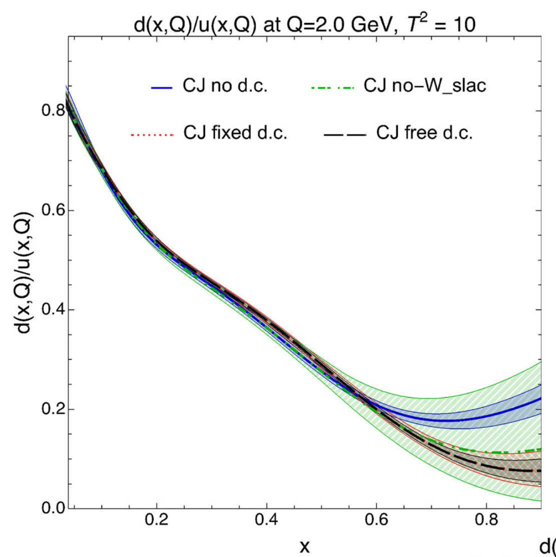

[Accardi et al, EPJC81]

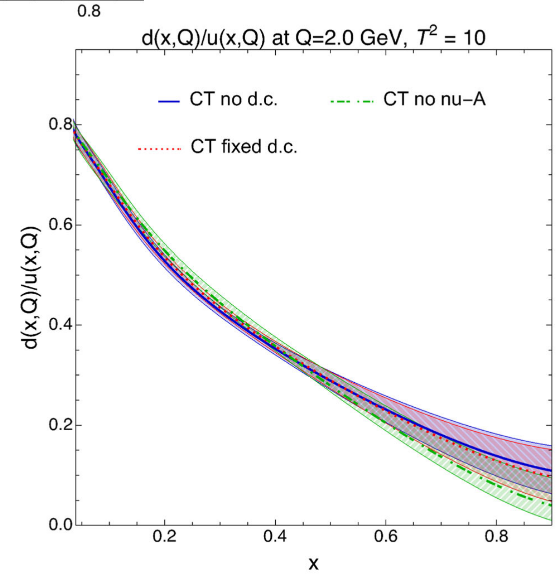

[Hou et al, PRD103]

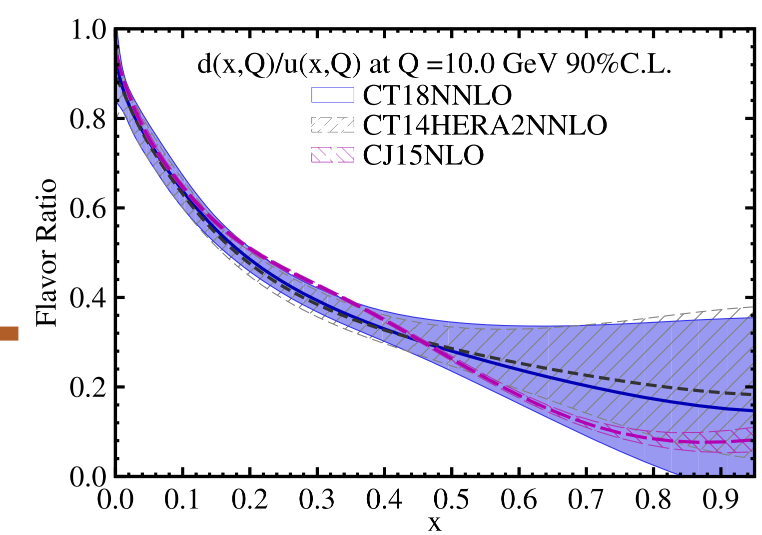

CT: role of parametrization, detailed uncertainties

Theoretical constraints and phenomenological analyses

We explore quark counting rules to probe large-x structure from QCD scattering data.

[AC & Nadolsky, PRD 103 (2021)]

Quark counting rules where proved for exclusive and inclusive processes.

They focus on the role of the struck quark when carrying most of the hadron momentum.

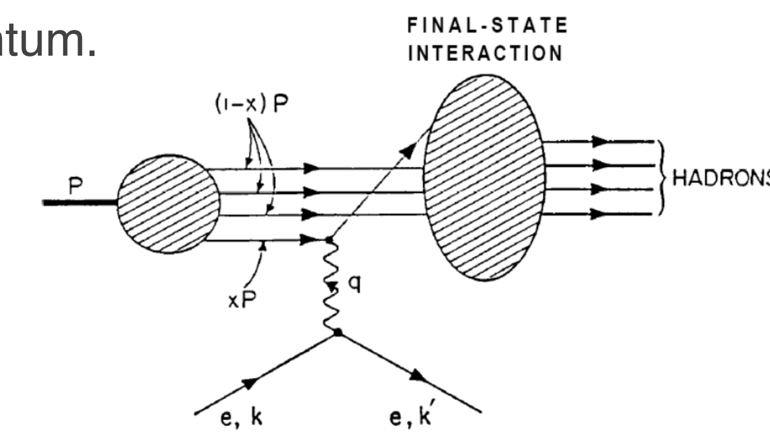

$$F_2(x_B) \xrightarrow[x_B \to 1]{} (1 - x_B)^{2p-1+2|\lambda_q - \lambda_A|}$$

$p = \#$ spectators
λ_q & λ_A = helicities of active quark and target

Brodsky and Farrar; Ezawa; Berger and Brodsky; Soper; Brodsky, Burkardt and Schmidt

Quark counting rules are often extended from structure functions to PDFs.

$$f(x) \xrightarrow[x_B \to 1]{} (1 - x_B)^{n=3} \qquad (1 - x_B)^{n>4} \qquad (1 - x_B)^{n>5}$$

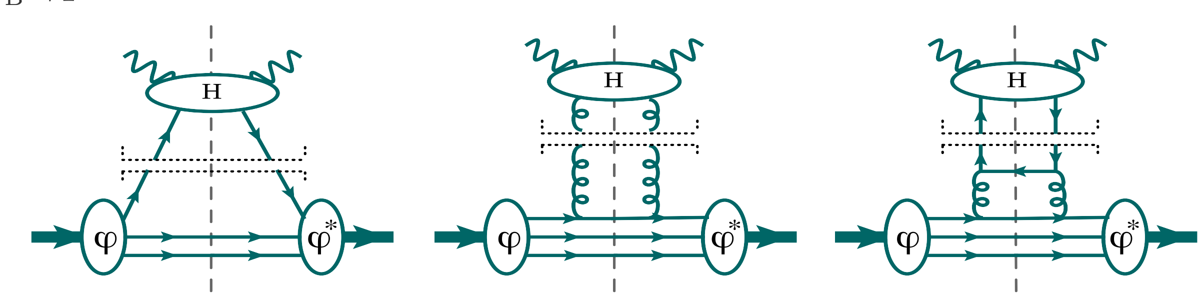

Analyze QCR with CT18NNLO global fit of proton PDFs,
explore the functional mimicry of PDFs and
revisit the interpretation of the "data vs. physical manifestations".

Effective exponents for structure functions and PDFs

[Ball et al, EPJC76]
[AC & Nadolsky, PRD 103 (2021)]

Baseline functional form in global analyses $f_{a/A}(x, Q_0^2) = x^{A_{1,a}}(1-x)^{A_{2,a}} \times \Phi_a(x)$

such that we can define: $\boxed{A_2^{\text{eff}}(F) \equiv \frac{\partial \ln (F(x,Q))}{\partial \ln (1-x)}}$

F_2 follows QCR within uncertainties.

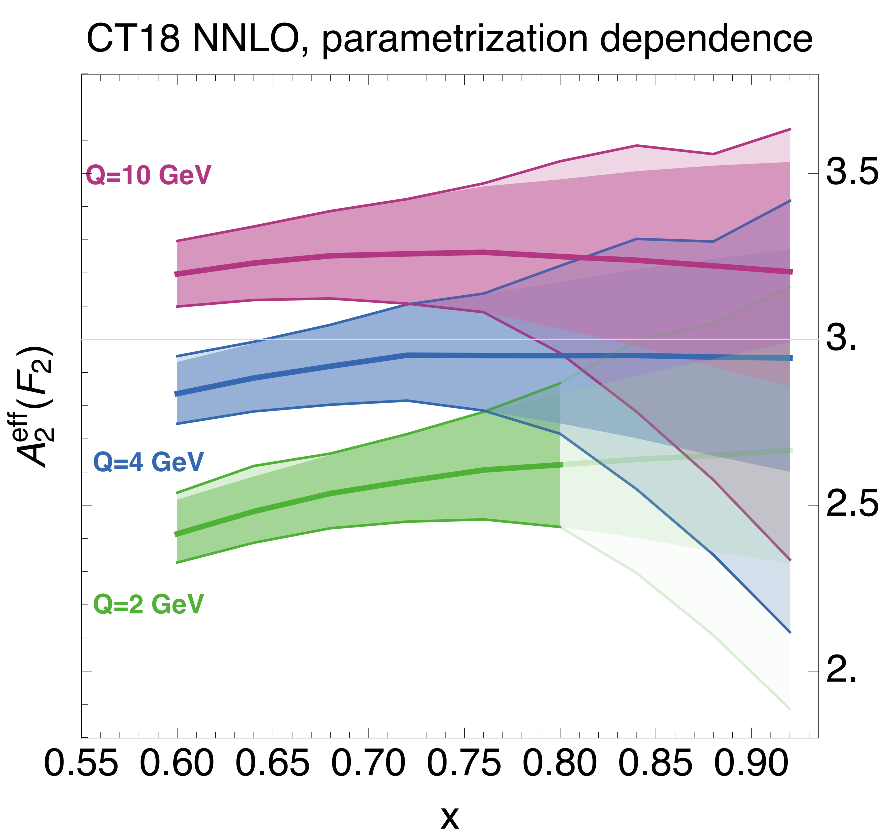

Valence PDFs are compatible with QCRs.

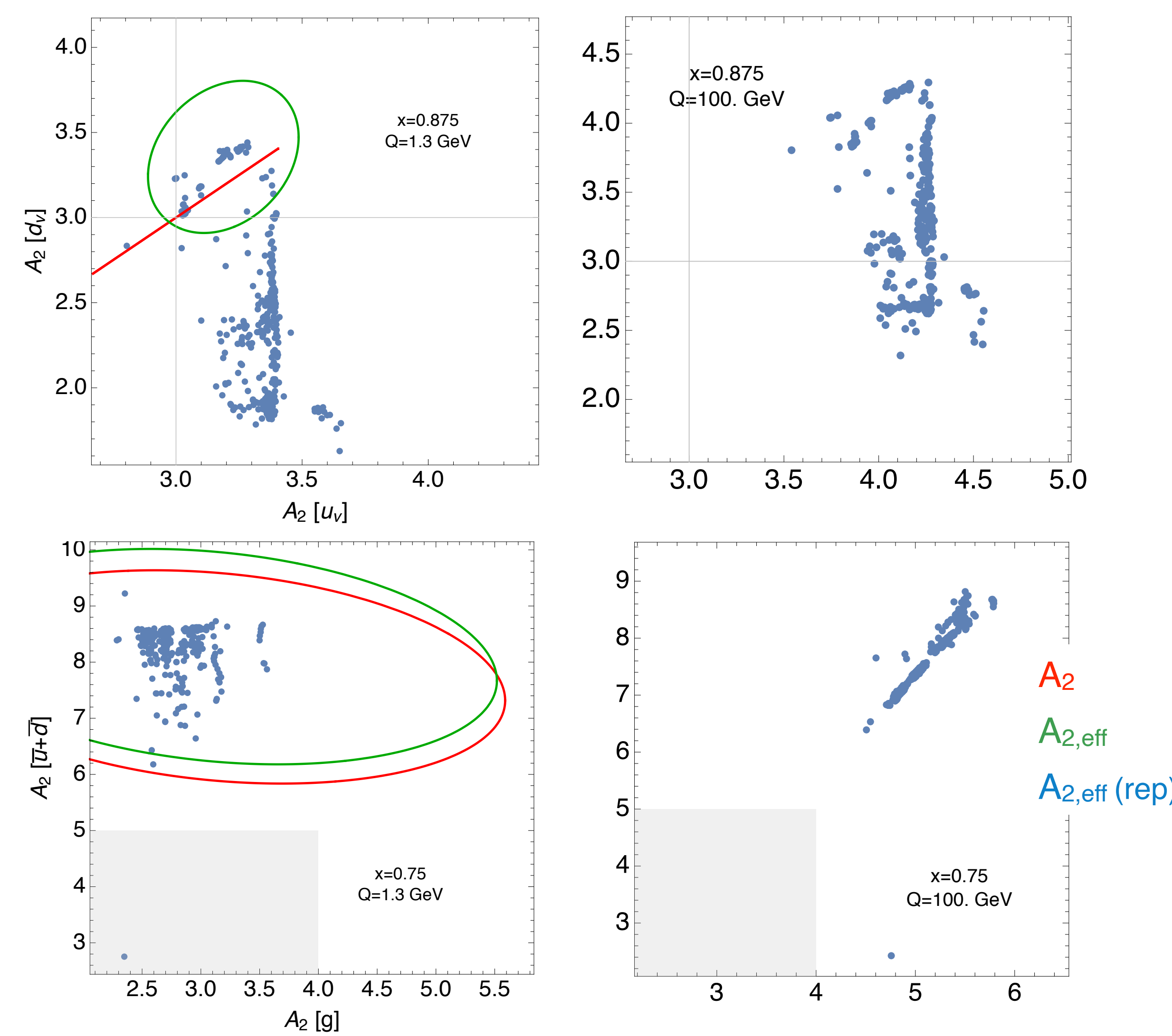

Pheno PDFs with different perspectives

Comparison of CTEQ-TEA (CT) and CTEQ-JLab (CJ) analyses

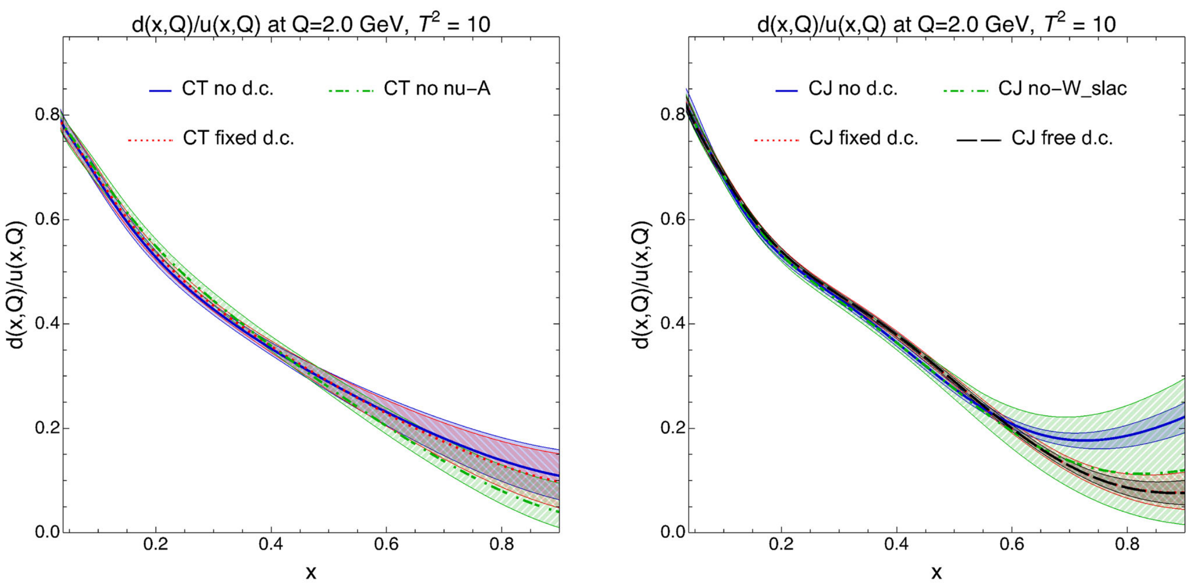

L$_2$ sensitivity shows the correlation between a given PDF configuration and objective function.

Pulls on χ^2 when $f(x) \to f(x) + \Delta f(x)$.

Pulls affected by cuts, e.g. on deuteron data sets

[Accardi et al, EPJC81]

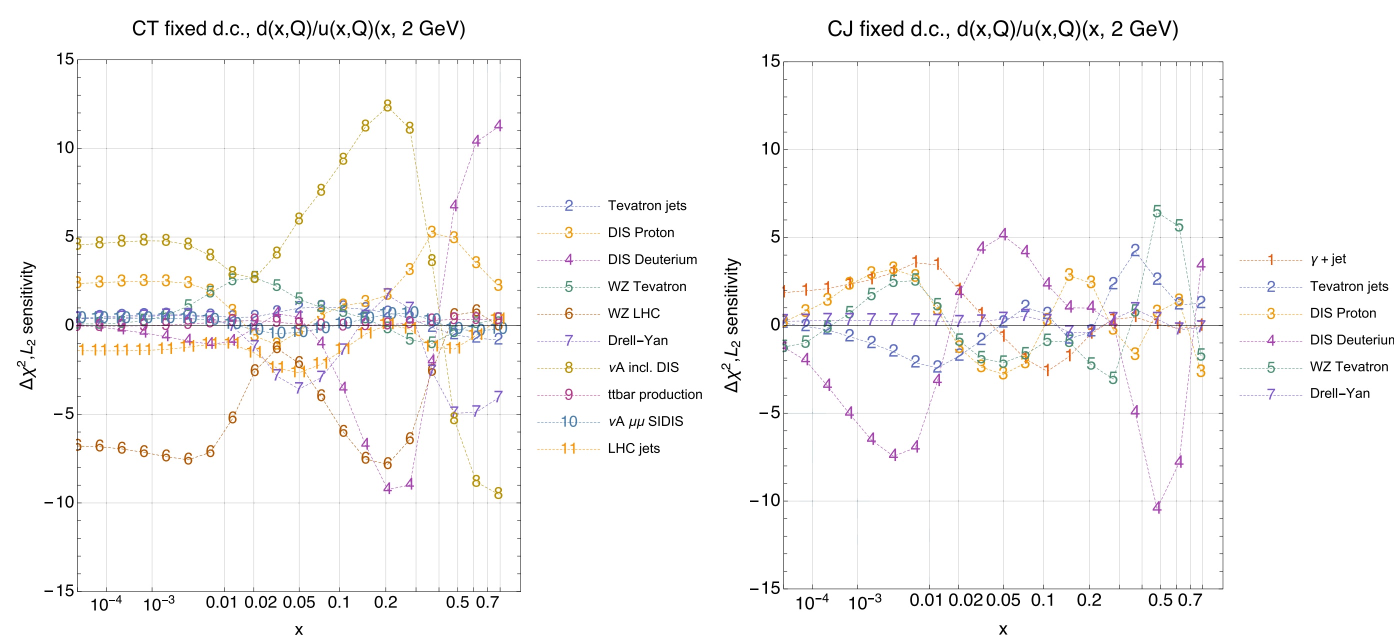

L$_2$ sensitivity: [Phys.Rev. D98 (2018)], [Phys.Rev.D 100 (2019)]